JOURNAL OF THERMOPHYSICS AND HEAT TRANSFER
Vol. 13, No. 4, October–December 1999

BGK–Burnett Equations for Flows in the Continuum-Transition Regime

Ramesh Balakrishnan,* Ramesh K. Agarwal,† and Keon-Young Yun‡
Wichita State University, Wichita, Kansas 67260-0093

To extend the range of applicability of continuum formulations into the continuum-transition regime, an extended set of fluid dynamic equations has been derived. These equations, termed as the Bhatnagar-Gross-Krook (BGK)-Burnett equations, have been derived by taking moments of the Boltzmann equation by using the BGK model for the collision integral. The second-order distribution function that forms the basis of this derivation is formulated by considering the first three terms of the Chapman-Enskog expansion. It is shown that the BGK–Burnett equations have been used to compute the hypersonic shock structure and the hypersonic flow past a blunt body. The results of these computations are compared with the augmented Burnett and Navier-Stokes solutions. The second-order distribution function does not violate Boltzmann's H-theorem; as a consequence the BGK–Burnett equations are entropy consistent for the range of Knudsen numbers for which computations have been performed.

Nomenclature

$\boldsymbol{C} = \boldsymbol{v} - \boldsymbol{u}$	= peculiar velocity vector
e_t	= specific total energy
f	= distribution function
$f^{(0)}$	= Maxwellian distribution
$f^{(1)} = f^{(0)}\phi^{(1)}$	= first-order component
$f^{(2)}$	= second-order component
$\boldsymbol{G}$	= x component of the flux vector
$\boldsymbol{H}$	= y component of the flux vector
I	= internal energy
$I_0 = \langle I, f^{(0)} \rangle$	= average internal energy
M_∞	= freestream Mach number
Pr	= Prandtl number
$\boldsymbol{Q}$	= field vector
$\dot{q}_i$	= heat flux
$\mathcal{R} = (-\infty, \infty)$	= real axis
$\mathcal{R}^+ = [0, \infty)$	= positive real axis
$\mathcal{R}^- = (-\infty, 0]$	= negative real axis
Re_∞	= freestream Reynolds number
$\boldsymbol{u}$	= fluid velocity vector
$\boldsymbol{v}$	= molecular velocity vector
$\bar{\alpha}$	= accomodation coefficient
$\alpha_{(i)}$	= second-order closure coefficients
$\beta = 1/2RT$	= reciprocal temperature
γ	= specific heat ratio
$\kappa = \mu\gamma R/(\gamma - 1)$	= thermal conductivity
λ	= mean free path
$\mu = p/\nu$	= molecular viscosity coefficient
ν	= molecular collision frequency
ξ	= Knudsen number
ρ	= density
$\dot{\sigma}$	= irreversible entropy production
$\bar{\sigma}$	= reflection coefficient
$\tau_{i,j}$	= stress tensor components
$\boldsymbol{\Psi}$	= collision invariant vector

Subscripts and Superscripts

a	= acoustic flux
B	= BGK–Burnett flux components
i	= Euler flux
s	= body surface
v	= Navier-Stokes flux components
x	= x component
y	= y component

Presented as Paper 97-2551 at the AIAA 32nd Thermophysics Conference, Atlanta, GA, 23–25 June 1997; received 7 August 1997; revision received 11 February 1999; accepted for publication 2 March 1999.

*Graduate Research Assistant, Department of Aerospace Engineering.
†Bloomfield Distinguished Professor and Executive Director, Department of Aerospace Engineering, National Institute for Aviation Research. Fellow AIAA.
‡Graduate Research Assistant, Department of Aerospace Engineering. Student Member AIAA.

I. Introduction

THE various portions of the flight envelope of space vehicles may be broadly classified into the continuum, continuum-transition, and free molecular regimes. The Boltzmann equation describes the properties of the fluid in all of these regimes. However, it is very difficult to obtain closed-form analytic solutions except for the simplest of flows, which are largely of academic interest. For practical problems, however, approximation techniques need to be applied to the Boltzmann equation in order to obtain meaningful solutions. The techniques available for solving the Boltzmann equation can be classified into particulate methods and moment methods. The direct simulation Monte Carlo (DSMC)[1] falls under the category of particulate methods, and the fluid dynamic equations [Euler, Navier–Stokes and Bhatnagar-Gross–Krook (BGK)–Burnett] fall under the class of moment methods. In the continuum regime the Knudsen number is relatively small, i.e., $Kn_\infty \ll 1$, as the mean free path is several orders of magnitude smaller than the characteristic length scale and the flow is collision dominated. The Euler and Navier–Stokes equations adequately model the properties of a fluid in this regime. In the free molecular flow regime the mean free path is several orders of magnitude greater than the characteristic length, i.e., $Kn_\infty \gg 1$, and the effects of intermolecular collisions are negligible. The DSMC technique, to simulate the Boltzmann equation, provides reasonable estimates for the flow variables in the free molecular regime. The most difficult regime is the continuum-transition regime where the mean free path is of the same order of magnitude as the characteristic length, i.e., $Kn_\infty \sim 1$. In this regime there are few model equations that are computationally tractable and also accurately predict the flow properties. The DSMC method is not suitable to compute the Boltzmann equation in this regime because of the large number densities needed to make the simulations meaningful. This makes the DSMC method prohibitively expensive in terms of computational work and storage requirements. Hence

there is a need for an extended set of governing equations that can perform equally well in the continuum and continuum-transition regimes.

In developing an extended set of equations, the following questions need to be addressed:

1) How do we formulate the constitutive relations for the stress and heat transfer that will be valid in the continuum and continuum-transition regimes?

2) How do we specify the boundary conditions, especially solid-wall boundary conditions for the new set of equations?

3) Can the numerical techniques available for the Navier–Stokes equations be extended to include the new constitutive relations?

One of the methods in this direction employs the Chapman–Enskog expansion to devise higher-order distribution functions. This expansion gives rise to the Navier–Stokes equations for first-order departures from collisional equilibrium. In an attempt to extend this expansion to higher orders, Burnett[2] developed constitutive relationships for the stress and heat-transfer terms by applying the Chapman–Enskog expansion to the Boltzmann equation for second-order departures from collisional equilibrium. These equations will be referred to as the *original* Burnett equations. In 1939 Chapman and Cowling[3] replaced the material derivatives in the original Burnett equations by spatial derivatives obtained from inviscid (Euler) equations. This alternate form of the original Burnett equations will be referred to, henceforth, as the *conventional* Burnett equations. The use of Euler equations to express the material derivatives retained the second-order accuracy of the Burnett equations. In recent years Fiscko and Chapman[4] and Zhong[5] have used the conventional Burnett equations to extend the numerical methods for continuum flow into the continuum-transition regime by incorporating the additional stress and heat-transfer terms in standard Navier–Stokes solvers. In an attempt to solve the conventional Burnett equations, Fiscko and Chapman[4] solved the hypersonic shock structure problem by relaxing an initial solution to steady state. They obtained solutions for a variety of Mach numbers and concluded that the conventional Burnett equations do indeed describe the normal shock structure better than the Navier–Stokes equations at high Mach numbers. They however experienced stability problems when they made the grids progressively finer, which was predicted by Bobylev,[6] who showed that the linearized conventional Burnett equations were unstable to small wavelength disturbances. In a subsequent attempt Zhong[5] showed that the conventional Burnett equations could be stabilized by adding linear third-order terms from the super-Burnett equations, thereby maintaining second-order accuracy. This set of equations was termed the *augmented* Burnett equations. The coefficients (weights) of these linear third-order terms were determined by carrying out a linearized stability analysis of the augmented Burnett equation. The augmented Burnett equations did not present any stability problems when they were used to compute the flow properties in the hypersonic shock structure and hypersonic blunt-body flows problems. However, attempts at computing blunt-body wakes and flat-plate boundary layers even with the augmented Burnett equations have not been entirely successful. Further, the ad hoc addition of linear super-Burnett terms and their necessity raises the question of whether the approximation used to create the conventional Burnett equations from the original Burnett equations introduces the small wavelength instabilities. Welder et al.[7] and Comeaux et al.[8] have noted that linear stability analysis alone is not sufficient to explain the instability of Burnett equations with increasing Knudsen numbers as this analysis does not take into account many nonlinear terms (products of flow variables and their derivatives) that are present in the conventional Burnett equations. Comeaux et al.[8] showed that this instability is because the conventional Burnett equations can violate the second law of thermodynamics at higher Knudsen numbers.

To understand the cause of these instabilities, it was decided to formulate a higher-order set of governing equations from first principles. The highly nonlinear nature of the collision integral in the Boltzmann equation presents the biggest hurdle in devising a second-order distribution function. This problem is circumvented by representing the collision integral in the BGK[1,9] form. This approximation assumes that any slight departure from the equilibrium (Maxwellian) distribution function will settle down to the equilibrium distribution exponentially. This approximation also assumes that the gas is dilute, and hence the collision process is predominantly binary in nature. A further implication of this assumption is that the time taken for the nonequilibrium distribution function to settle down to equilibrium levels is equal to the reciprocal of the collision frequency. The exact closed-form analytical expression for the distribution function is derived by considering the first three terms of the Chapman–Enskog expansion. Moments of the BGK–Boltzmann equation, with the collision invariant vector, using this distribution function give rise to the BGK–Burnett equations.[10–12] In this formulation we assume that the molecules are hard elastic spheres with no intermolecular forces acting between them. An important feature of the second-order formulation is the appearance of material derivatives in the stress and heat-transfer terms in the BGK–Burnett flux vectors. These can be expressed in terms of spatial derivatives by using either the Euler or Navier–Stokes equations. When the Navier–Stokes equations are used to express the material derivatives, the resulting BGK–Burnett equations are unconditionally stable to a wide range of local Knudsen numbers.

The hypersonic shock structure was computed with the one-dimensional BGK–Burnett equations, and Ref. 11 has shown that these equations did not exhibit the small wavelength instability characteristic of the conventional Burnett equations. To check whether the entropy production is positive throughout the flowfield, the Boltzmann's H-theorem was applied to the second-order distribution function. The modified $\mathcal{H}$ function derived by Deshpande[13] has been used to show that the irreversible entropy produced by the one-dimensional BGK–Burnett equations is positive for a wide range of Knudsen numbers for which computations have been carried out.

The hypersonic flowfield about a cylindrical leading edge was computed with the two-dimensional BGK–Burnett equations. Computations were carried out for freestream Knudsen numbers $Kn_\infty = 0.001$ and 0.01. A grid-convergence study showed that the two-dimensional BGK–Burnett equations, once again, did not exhibit any small wavelength instability when the mesh was refined.

II. One-Dimensional BGK–Burnett Equations

A closed-form expression for the second-order distribution function is obtained by considering the first three terms of the Chapman–Enskog expansion given by

$$f = f^{(0)} + \xi f^{(1)} + \xi^2 f^{(2)} \tag{1}$$

where $f^{(0)}$ denotes the equilibrium (Maxwellian) distribution function[§]:

$$f^{(0)} = (\rho/I_0)\sqrt{(\beta/\pi)}\exp\left[-I/I_0 - \beta C_x^2\right] \tag{2}$$

and $f^{(i)}$, $\forall i = 1, 2, \ldots, \infty$, higher-order components of the distribution function. On substituting Eq. (1) in the one-dimensional BGK–Boltzmann equation[¶]:

$$\frac{\partial f}{\partial t} + v_x \frac{\partial f}{\partial x} = \nu\left(f^{(0)} - f\right) \tag{3}$$

and equating like powers of the Knudsen number, we obtain the

[§]This form of the Maxwellian distribution function considers the energy contribution from the various nontranslational modes of freedom. All of these contributing factors are grouped together in the so-called internal energy term I. This term can be shown to reduce to zero for the special case of a monatomic gas. The original derivation of the Burnett equations considers the molecules, comprising the gas, to consist of only translational modes of energy. The inclusion of the internal energy term allows this formulation to be used for monatomic as well as polyatomic gases.

[¶]The molecular collision frequency ν is assumed to be independent of the molecular velocity.

following equation for the higher-order components of the distribution function:

$$f^{(i)} = -\frac{1}{\xi\nu}\left[\frac{\partial f^{(i-1)}}{\partial t} + v_x\frac{\partial f^{(i-1)}}{\partial x}\right] \tag{4}$$

$\forall i = 1, 2, \ldots, \infty$. On expressing $f^{(1)} = f^{(0)}\phi^{(1)}$ and using the one-dimensional Euler equations to express the temporal derivatives in terms of the spatial derivatives,[10] we obtain

$$f^{(1)} = f^{(0)}\phi^{(1)} = -\frac{f^{(0)}}{\xi\nu}\left[\mathcal{A}^{(1)}(I, C_x)\frac{\partial\beta}{\partial x} + \mathcal{A}^{(2)}(I, C_x)\frac{\partial u_x}{\partial x}\right] \tag{5}$$

where v_x, $C_x = v_x - u_x$, and u_x denote the x component of the molecular, peculiar or thermal, and fluid velocities, respectively. I denotes the internal energy (energy due to nontranslational degrees of freedom), $I_0 = (3-\gamma)/[4\beta(\gamma-1)]$ denotes the average internal energy,** and $\beta = 1/2RT$:

$$\mathcal{A}^{(1)}(I, C_x) = (5/2\beta)C_x - (I/\beta I_0)C_x - C_x^3 \tag{6}$$

$$\mathcal{A}^{(2)}(I, C_x) = (3-\gamma)\beta C_x^2 - (\gamma-1)\frac{I}{I_0} + \frac{(3\gamma-5)}{2} \tag{7}$$

The first-order component of the distribution function satisfies the moment closure relation

$$\left\langle \boldsymbol{\Psi}, \xi f^{(1)}\right\rangle = \left\langle \boldsymbol{\Psi}, \xi f^{(0)}\phi^{(1)}\right\rangle = 0 \tag{8}$$

where the inner product is defined as

$$\left\langle \boldsymbol{\Psi}, \xi f^{(1)}\right\rangle = \int_{\mathcal{R}^+}\int_{\mathcal{R}} \boldsymbol{\Psi}\xi f^{(1)}\,\mathrm{d}v_x I \tag{9}$$

$$\boldsymbol{\Psi} = \left[1, v_x, \left(I + v_x^2/2\right)\right]^T \tag{10}$$

denotes the collision invariant vector. The physical implication of this relation is that the first-order term of the distribution function does not add any additional terms to the field vector $\boldsymbol{Q}$ of the conservation equations. This property will be used in deriving a closed-form expression for the second-order distribution function.

On substituting for $f^{(1)}$ in Eq. (4), we obtain

$$f^{(2)} = -\frac{1}{\xi\nu}\left\{\frac{\partial}{\partial t}\left[f^{(0)}\phi^{(1)}\right] + \frac{\partial}{\partial x}\left[u_x f^{(0)}\phi^{(1)}\right] + \frac{\partial}{\partial x}\left[C_x f^{(0)}\phi^{(1)}\right]\right\} \tag{11}$$

The second-order term $f^{(2)}$ in the distribution function must satisfy the moment closure relationship

$$\left\langle \boldsymbol{\Psi}, \xi^2 f^{(2)}\right\rangle = 0 \tag{12}$$

On substituting for $f^{(2)}$ from Eq. (11), we obtain

$$\left\langle \boldsymbol{\Psi}, \xi^2 f^{(2)}\right\rangle = -\frac{\xi^2}{\xi\nu}\left[\frac{\partial}{\partial t}\left\langle \boldsymbol{\Psi}, f^{(0)}\phi^{(1)}\right\rangle + \frac{\partial}{\partial x}\left\langle \boldsymbol{\Psi}, u_x f^{(0)}\phi^{(1)}\right\rangle + \frac{\partial}{\partial x}\left\langle \boldsymbol{\Psi}, C_x f^{(0)}\phi^{(1)}\right\rangle\right] \tag{13}$$

A. Moment Closure Functions and Coefficients

From Eq. (13) one can see that the moments $\langle \boldsymbol{\Psi}, C_x f^{(0)}\phi^{(1)}\rangle$ are not equal to zero.†† Hence, we need to define some additional terms with closure coefficients that satisfy the moment closure relationship (12). In the formulation of the second-order distribution function, the form of the additional terms in the moment closure functions was chosen‡‡ to be similar to the functions in $\mathcal{A}^{(i)}(I, C_x)$. Each of these additional terms was weighted, and the magnitudes of these weights were determined by solving Eq. (12). The second-order term $f^{(2)}$ is defined as

$$f^{(2)} = -\frac{1}{\xi\nu}\left\{\frac{\partial}{\partial t}\left[f^{(0)}\phi^{(1)}\right] + \frac{\partial}{\partial x}\left[u_x f^{(0)}\phi^{(1)}\right] + \frac{\partial}{\partial x}\left[f^{(0)}\tilde{\phi}^{(1)}(I, C_x)\right]\right\} \tag{14}$$

where

$$\tilde{\phi}^{(1)}(I, C_x) = -\frac{1}{\xi\nu}\left[\tilde{\mathcal{A}}^{(1)}(I, C_x)\frac{\partial\beta}{\partial x} + \tilde{\mathcal{A}}^{(2)}(I, C_x)\frac{\partial u_x}{\partial x}\right] \tag{15}$$

The moment closure functions $\tilde{\mathcal{A}}^{(i)}(I, C_x)$, $\forall i = 1, 2$ in Eq. (15) are defined as

$$\tilde{\mathcal{A}}^{(1)}(I, C_x) = (\theta_1/\beta)C_x + (\theta_2/\beta I_0)IC_x + \theta_3 C_x^3 \tag{16}$$

$$\tilde{\mathcal{A}}^{(2)}(I, C_x) = \beta\theta_4 C_x^2 + \theta_5(I/I_0) + \theta_6 \tag{17}$$

The closure coefficients θ_i $\forall i = 1, \ldots, 6$ are given in the Appendix.

B. One-Dimensional BGK–Burnett Stress and Heat-Transfer Terms

The BGK–Burnett equations are obtained by taking moments of the BGK–Boltzmann equation with the collision invariant vector $\boldsymbol{\Psi}$, using the second-order distribution function. The BGK–Burnett equations are represented in the conservation law form as

$$\frac{\partial \boldsymbol{Q}}{\partial t} + \frac{\partial \boldsymbol{G}}{\partial x} = 0 \tag{18}$$

where $\boldsymbol{G} = \boldsymbol{G}^i + \boldsymbol{G}^v + \boldsymbol{G}^B$. The field vector $\boldsymbol{Q}$ and component vectors of the flux vector $\boldsymbol{G}$ are

$$\boldsymbol{Q} = \begin{bmatrix}\rho\\ \rho u_x\\ \rho e_t\end{bmatrix}, \qquad \boldsymbol{G}^i = \begin{bmatrix}\rho u_x\\ p + \rho u_x^2\\ p u_x + \rho u_x e_t\end{bmatrix}$$

$$\boldsymbol{G}^v = \begin{bmatrix}0\\ -\tau_{xx}^v\\ -u_x\tau_{xx}^v + \dot{q}_x^v\end{bmatrix}, \qquad \boldsymbol{G}^B = \begin{bmatrix}0\\ -\tau_{xx}^B\\ -u_x\tau_{xx}^B + \dot{q}_x^B\end{bmatrix}$$

The Navier–Stokes stress and heat-transfer terms in the flux vectors are given by

$$\tau_{xx}^v = (3-\gamma)\mu\frac{\partial u_x}{\partial x} \tag{19}$$

$$\dot{q}_x^v = -\kappa\frac{\partial T}{\partial x} \tag{20}$$

where $\mu = p/\nu$ and $\kappa = \mu R[\gamma/(\gamma-1)]$. The BGK–Burnett stress and heat-transfer terms are given by

$$\tau_{xx}^B = -\Omega_1\frac{\rho}{\beta\nu^2}\frac{\mathbf{D}}{\mathbf{D}t}\left(\frac{\partial u_x}{\partial x}\right) + \Omega_1\frac{\rho}{\beta^2\nu^2}\left(\frac{\partial u_x}{\partial x}\right)\frac{\mathbf{D}\beta}{\mathbf{D}t} - \Omega_2\frac{1}{\beta^3\nu^2} \times \left(\frac{\partial\rho}{\partial x}\right)\left(\frac{\partial\beta}{\partial x}\right) - \Omega_2\frac{\rho}{\beta^3\nu^2}\left(\frac{\partial^2\beta}{\partial x^2}\right) + 3\Omega_2\frac{\rho}{\beta^4\nu^2}\left(\frac{\partial\beta}{\partial x}\right)^2 \tag{21}$$

**This denotes the average internal energy in one dimension.

††These moments in fact give rise to the flux vectors in the Navier–Stokes equations.

‡‡Since the only relation available to determine the magnitudes of the weights is the moment closure relation, Eq. (12), we must note that a unique formulation of the second-order distribution function is not possible. By assuming the form of the moment closure relations to be similar to the functions $\mathcal{A}^{(i)}(I, C_x)$, we are imposing an additional constraint in order to close the system of equations.

$$\dot{q}_x^B = \Omega_1 \frac{\rho}{\beta\nu^2}\left(\frac{\partial u_x}{\partial x}\right)\frac{\mathbf{D}u_x}{\mathbf{D}t} - \Omega_3 \frac{\rho}{\beta^3\nu^2}\frac{\mathbf{D}}{\mathbf{D}t}\left(\frac{\partial \beta}{\partial x}\right) + 3\Omega_3 \frac{\rho}{\beta^4\nu^2}\left(\frac{\partial \beta}{\partial x}\right)\frac{\mathbf{D}\beta}{\mathbf{D}t} + \Omega_4 \frac{1}{\beta^2\nu^2}\left(\frac{\partial \rho}{\partial x}\right)\left(\frac{\partial u_x}{\partial x}\right) + (\Omega_2 - 2\Omega_4)\frac{\rho}{\beta^3\nu^2}\left(\frac{\partial u_x}{\partial x}\right)\left(\frac{\partial \beta}{\partial x}\right) + \Omega_4 \frac{\rho}{\beta^2\nu^2}\left(\frac{\partial^2 u_x}{\partial x^2}\right) \quad (22)$$

On using the Navier–Stokes equations to express the material derivatives,[§§] in terms of the spatial derivatives, the stress and heat flux terms in the BGK–Burnett flux vector take the form

$$\tau_{xx}^B = -\frac{\mu^2}{p}\left[a_1\left(\frac{\partial u_x}{\partial x}\right)^2 + a_2\frac{T}{\rho}\left(\frac{\partial^2 \rho}{\partial x^2}\right) + a_3\frac{T}{\rho^2}\left(\frac{\partial \rho}{\partial x}\right)^2 + a_4\frac{1}{\rho}\left(\frac{\partial \rho}{\partial x}\right)\left(\frac{\partial T}{\partial x}\right) + a_5\frac{1}{T}\left(\frac{\partial T}{\partial x}\right)^2 + a_6\frac{\partial^2 T}{\partial x^2}\right] - \frac{\mu^3}{p^2}\left[a_7\frac{T}{\rho}\left(\frac{\partial \rho}{\partial x}\right)\left(\frac{\partial^2 u_x}{\partial x^2}\right) + a_8\left(\frac{\partial u_x}{\partial x}\right)\left(\frac{\partial^2 T}{\partial x^2}\right) + a_9 T\left(\frac{\partial^3 u_x}{\partial x^3}\right) + a_{10}\left(\frac{\partial u_x}{\partial x}\right)^3\right] \quad (23)$$

$$\dot{q}_x^B = \frac{\mu^2}{\rho}\left[b_1\frac{1}{T}\left(\frac{\partial u_x}{\partial x}\right)\left(\frac{\partial T}{\partial x}\right) + b_2\left(\frac{\partial^2 u_x}{\partial x^2}\right) + b_3\frac{1}{\rho}\left(\frac{\partial \rho}{\partial x}\right)\left(\frac{\partial u_x}{\partial x}\right)\right] + \frac{\mu^3}{p\rho}\left[b_4\left(\frac{\partial u_x}{\partial x}\right)\left(\frac{\partial^2 u_x}{\partial x^2}\right) + b_5\frac{1}{T}\left(\frac{\partial T}{\partial x}\right)\left(\frac{\partial^2 T}{\partial x^2}\right) + b_6\frac{1}{\rho}\left(\frac{\partial \rho}{\partial x}\right)\left(\frac{\partial^2 T}{\partial x^2}\right) + b_7\left(\frac{\partial^3 T}{\partial x^3}\right) + b_8\frac{1}{T}\left(\frac{\partial T}{\partial x}\right)\left(\frac{\partial u_x}{\partial x}\right)^2 + b_9\frac{1}{\rho}\left(\frac{\partial \rho}{\partial x}\right)\left(\frac{\partial u_x}{\partial x}\right)^2 + b_{10}\frac{1}{T^2}\left(\frac{\partial T}{\partial x}\right)^3\right] \quad (24)$$

The expressions for the BGK–Burnett stress and heat transfer, Eqs. (23) and (24), contain terms that are $\mathcal{O}(\mu^2)$ and $\mathcal{O}(\mu^3)$. Terms of $\mathcal{O}(\mu^2)$ are obtained when the Euler equations are used to express the material derivatives. The additional terms that are of $\mathcal{O}(\mu^3)$ result when the Navier–Stokes equations are used to express the material derivatives. The coefficients $\Omega_1 \cdots \Omega_4$, $a_1 \cdots a_{10}$, and $b_1 \cdots b_{10}$ are functions of $\theta_i \; \forall\, i = 1, 2, \ldots, 6$ and can be obtained by expressing the material derivatives in terms of the spatial derivatives and simplifying the resulting expressions.

III. Linearized Stability Analysis

Bobylev[6] showed that the conventional Burnett equations are not stable to small wavelength disturbances. Hence the conventional Burnett equations tend to blow up when the mesh size is made progressively finer. To investigate the stability aspects of the BGK–Burnett equations, a model problem is considered, which studies the response of a uniform gas to a one-dimensional periodic perturbation wave. An intuitive notion of stability requires that a mathematical model of a system when subjected to small perturbations responds in a manner such that the effects of these perturbations become vanishingly small over a finite period of time. Since the perturbations are assumed to be small, only linear terms need be considered for the purpose of analysis. To check whether the BGK–Burnett equations are stable, this simple analytical analysis is carried out by linearizing the equations. The response of these linearized BGK–Burnett equations is shown to be stabilizing for a wide range of Knudsen numbers.

A. Case 1

The density ρ and temperature T of the undisturbed gas at time $t = 0$ are ρ_0 and T_0, respectively. At time $t = 0$ the gas is perturbed such that $\rho = \rho_0[1 + C_1 \exp(i\omega x/L_0)]$, $T = T_0[1 + C_2 \exp(i\omega x/L_0)]$ and $u_x = \sqrt{(RT_0)}[C_3 \exp(i\omega x/L_0)]$. Since the perturbations are assumed to be small, the magnitudes of the C_k in Eqs. (25)–(27) are required to satisfy the inequality $|C_k| \ll 1, \; \forall k = 1, \ldots, 3$. The characteristic length $L_0 = \mu_0/\rho_0\sqrt{(RT_0)} = 0.783\lambda$. The nondimensional circular frequency $\omega = 2\pi L_0/L = 4.92(\lambda/L) = 4.92Kn$. On introducing the perturbed quantities in the continuity, momentum and energy equations, and neglecting products and powers of the flow variables and their derivatives, the following equations are obtained:

$$\frac{\partial \rho}{\partial t} + \rho\frac{\partial u_x}{\partial x} = 0 \quad (25)$$

$$\frac{\partial u_x}{\partial t} + R\frac{\partial T}{\partial x} + \frac{RT}{\rho}\frac{\partial \rho}{\partial x} - \frac{1}{\rho}\frac{\partial \tau_{xx}}{\partial x} = 0 \quad (26)$$

$$\frac{\partial T}{\partial t} + \frac{RT}{C_v}\frac{\partial u_x}{\partial x} + \frac{1}{\rho C_v}\frac{\partial \dot{q}_x}{\partial x} = 0 \quad (27)$$

The nondimensional density, temperature, velocity, distance, and time are defined as $\rho' = (\rho - \rho_0)/\rho_0$, $T' = (T - T_0)/T_0$, $u_x' = u_x/\sqrt{(RT_0)}$, $x' = x/L_0$, and $t' = tp_0/\mu_0$. On introducing these nondimensional variables, the continuity, momentum, and energy equations take the form

$$\frac{\partial \rho'}{\partial t'} + \frac{\partial u_x'}{\partial x'} = 0 \quad (28)$$

$$\frac{\partial u_x'}{\partial t'} + \frac{\partial \rho'}{\partial x'} + \frac{\partial T'}{\partial x'} - \frac{1}{\rho_0 RT_0}\frac{\partial \tau_{xx}}{\partial x'} = 0 \quad (29)$$

$$\frac{\partial T'}{\partial t'} + \frac{R}{C_v}\frac{\partial u_x'}{\partial x'} + \frac{\sqrt{RT_0}}{C_v R\rho_0 T_0^2}\frac{\partial \dot{q}_x}{\partial x'} = 0 \quad (30)$$

On substituting for τ_{xx} and $\dot{q}_x$ from the BGK–Burnett equations, the following equations are obtained:

$$\frac{\partial \rho'}{\partial t'} + \frac{\partial u_x'}{\partial x'} = 0 \quad (31)$$

$$\frac{\partial u_x'}{\partial t'} + \frac{\partial \rho'}{\partial x'} + \frac{\partial T'}{\partial x'} - (3-\gamma)\frac{\partial^2 u_x'}{\partial x'^2} + a_2'\frac{\partial^3 \rho'}{\partial x'^3} + a_6'\frac{\partial^3 T'}{\partial x'^3} + a_9'\frac{\partial^4 u_4'}{\partial x'^4} = 0 \quad (32)$$

$$\frac{\partial T'}{\partial t'} + (\gamma - 1)\frac{\partial u_x'}{\partial x'} + b_2(\gamma - 1)\frac{\partial^3 u_x'}{\partial x'^3} - \gamma\frac{\partial^2 T'}{\partial x'^2} + b_7(\gamma - 1)\frac{\partial^4 T'}{\partial x'^4} = 0 \quad (33)$$

where the superscript $'$ indicates normalization of these coefficients by the gas constant R. These equations can be cast in the form of a vector equation as

$$\frac{\partial \boldsymbol{V}'}{\partial t'} + \boldsymbol{M}_1\frac{\partial \boldsymbol{V}'}{\partial x'} + \boldsymbol{M}_2\frac{\partial^2 \boldsymbol{V}'}{\partial x'^2} + \boldsymbol{M}_3\frac{\partial^3 \boldsymbol{V}'}{\partial x'^3} + \boldsymbol{M}_4\frac{\partial^4 \boldsymbol{V}'}{\partial x'^4} = 0 \quad (34)$$

[§§] The material derivative is defined as $\mathbf{D}/\mathbf{D}t = \partial/\partial t + u_i(\partial/\partial x_i)$.

where

$$\boldsymbol{V}' = \begin{Bmatrix} \rho' \\ u_x' \\ T' \end{Bmatrix}, \qquad \boldsymbol{M}_1 = \begin{bmatrix} 0 & 1 & 0 \\ 1 & 0 & 1 \\ 0 & (\gamma-1) & 0 \end{bmatrix}$$

$$\boldsymbol{M}_2 = \begin{bmatrix} 0 & 0 & 0 \\ 0 & -(3-\gamma) & 0 \\ 0 & 0 & \gamma \end{bmatrix}, \qquad \boldsymbol{M}_3 = \begin{bmatrix} 0 & 0 & 0 \\ a_2' & 0 & a_6' \\ 0 & b_2(\gamma-1) & 0 \end{bmatrix}$$

$$\boldsymbol{M}_4 = \begin{bmatrix} 0 & 0 & 0 \\ 0 & a_9' & 0 \\ 0 & 0 & b_7'(\gamma-1) \end{bmatrix}$$

We assume the solution of Eq. (34) to be of the form

$$\boldsymbol{V}' = \bar{\boldsymbol{V}} e^{i\omega x'} e^{\phi t'} \tag{35}$$

where $\phi = \alpha + i\beta$ and α and β denote the attenuation and dispersion coefficients, respectively. The initial conditions for Eq. (34) can be denoted in vector form as $\boldsymbol{V}'|_{t=0} = \bar{\boldsymbol{V}} e^{i\omega x'}$. For stability $\alpha \le 0$ as L decreases, or in other words the flow must attenuate as the local Knudsen number increases. Substituting Eq. (35) in Eq. (34) and simplifying yields

$$\left[\phi \boldsymbol{I} + i\omega \boldsymbol{M}_1 - \omega^2 \boldsymbol{M}_2 - i\omega^3 \boldsymbol{M}_3\right] \boldsymbol{V}_0 e^{i\omega x'} e^{\phi t'} = 0 \tag{36}$$

when the Euler equations are used to express the material derivatives. For a nontrivial solution

$$\left|\phi \boldsymbol{I} + i\omega \boldsymbol{M}_1 - \omega^2 \boldsymbol{M}_2 - i\omega^3 \boldsymbol{M}_3\right| = 0 \tag{37}$$

Using the Navier–Stokes equations to express the material derivatives in terms of the spatial derivatives results in

$$\left[\phi \boldsymbol{I} + i\omega \boldsymbol{M}_1 - \omega^2 \boldsymbol{M}_2 - i\omega^3 \boldsymbol{M}_3 + \omega^4 \boldsymbol{M}_4\right] \boldsymbol{V}_0 e^{i\omega x'} e^{\phi t'} = 0 \tag{38}$$

For a nontrivial solution

$$\left|\phi \boldsymbol{I} + i\omega \boldsymbol{M}_1 - \omega^2 \boldsymbol{M}_2 - i\omega^3 \boldsymbol{M}_3 + \omega^4 \boldsymbol{M}_4\right| = 0 \tag{39}$$

The trajectory of the roots of the characteristic equations (37) and (39) are plotted on the complex plane on which the real axis denotes the attenuation coefficient and the imaginary axis denotes the dispersion coefficient. For stability it is required that the roots lie to the left of the imaginary axis as the local Knudsen number increases. Figures 1–4 show the trajectory of the roots of the characteristic equation as the Knudsen number increases. From the plots it is observed that when the Euler equations are used to approximate the

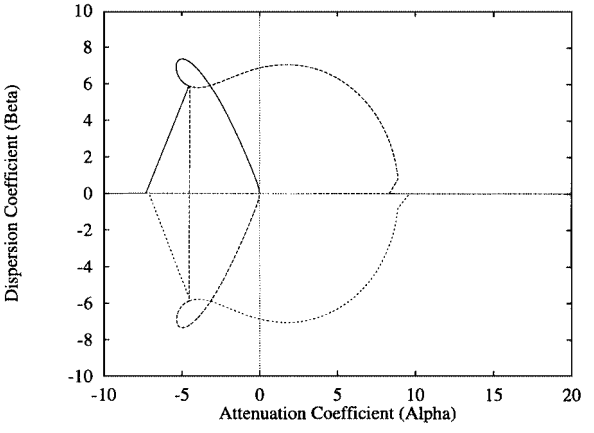

Fig. 1 Stability plot of the linearized BGK–Burnett equations in which Euler equations have been used to express the material derivatives, i.e., D( )/Dt, in terms of spatial derivatives. The $\gamma = 1.40$ (polyatomic gas, e.g., air), and $Pr = 1.0$. This plot shows that the BGK–Burnett equations are unconditionally stable when the internal energy contribution is nonzero.

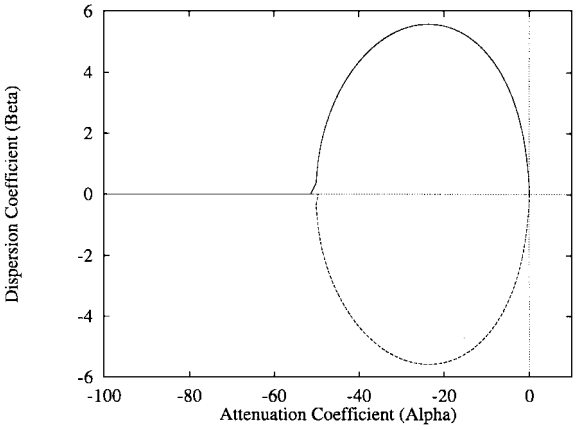

Fig. 2 Stability plot of the linearized BGK–Burnett equations in which Navier–Stokes equations have been used to express the material derivatives, i.e., D( )/Dt, in terms of spatial derivatives. The $\gamma = 1.40$ (polyatomic gas, e.g., air), and $Pr = 1.0$. This plot shows that the BGK–Burnett equations are unconditionally stable when the internal energy terms are nonzero.

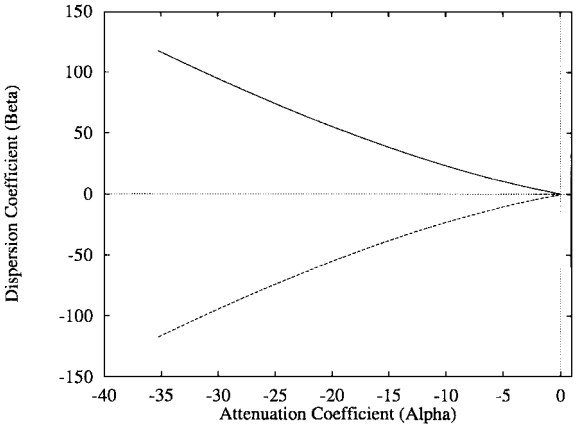

Fig. 3 Stability plot of the linearized BGK–Burnett equations in which Euler equations have been used to express the material derivatives, i.e., D( )/Dt, in terms of spatial derivatives. The $\gamma = 1.666$ (monatomic gas e.g., air), and $Pr = 1.0$. This plot shows that the BGK–Burnett equations are unconditionally stable when the internal energy contribution is zero.

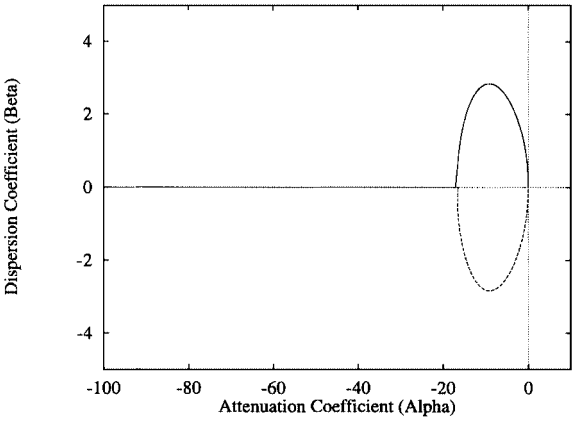

Fig. 4 Stability plot of the linearized one-dimensional BGK–Burnett equations in which the one-dimensional Navier–Stokes equations have been used to approximate the material derivatives, i.e., D( )/Dt, in terms of spatial derivatives. The $\gamma = 1.666$ (monatomic gas, e.g., argon), and $Pr = 1.0$. This plot shows that the BGK–Burnett equations are unconditionally stable.

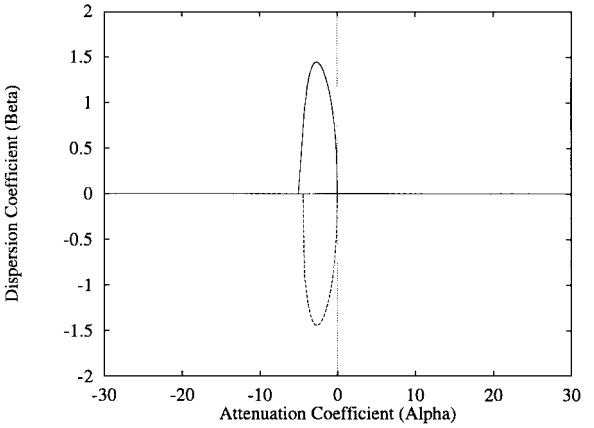

Fig. 5 Stability plot of the exact linearized BGK–Burnett equations in which no approximation has been used to express the material derivatives, i.e., D( )/Dt, in terms of spatial derivatives. The $\gamma = 1.666$ (monatomic gas, e.g., argon), and $Pr = 1.0$. The exact BGK–Burnett equations are unstable above a certain critical local Knudsen number. This plot suggests the need for approximating D( )/Dt.

material derivatives the BGK–Burnett equations are stable only for monatomic gases. For polyatomic gases such as air, it is observed that one of the roots of the characteristic equation assumes greater positive values when the local Knudsen number increases. However, unconditional stability for any gas is guaranteed when the Navier–Stokes equations are used to approximate the material derivatives.

B. Case 2

To check if the approximations introduced in expressing the material derivatives tend to destabilize the exact BGK–Burnett equations, the exact equations are linearized to yield

$$\left\{\begin{array}{c} \dfrac{\partial \rho'}{\partial t'} \\ \dfrac{\partial}{\partial t'}\left[u'_x + (3-\gamma)\dfrac{\partial^2 u'}{\partial x'^2}\right] \\ \dfrac{\partial}{\partial t'}\left[T' + \gamma\dfrac{\partial^2 T'}{\partial x'^2}\right] \end{array}\right\} + \boldsymbol{M}_1\frac{\partial \boldsymbol{V}'}{\partial x'} + \boldsymbol{M}_2\frac{\partial^2 \boldsymbol{V}'}{\partial x'^2} + \boldsymbol{M}_5\frac{\partial^3 \boldsymbol{V}'}{\partial x'^3} = 0 \tag{40}$$

The matrix $\boldsymbol{M}_5$ is given by

$$\begin{bmatrix} 0 & 0 & 0 \\ 0 & 0 & -3\left(\theta_1 + \theta_2 + \frac{5}{3}\theta_3\right) \\ 0 & \frac{1}{2}[\theta_4(6\gamma-3) + \theta_5(3+\gamma) + \theta_6(2\gamma)] & 0 \end{bmatrix} \tag{41}$$

The trajectory of the roots of the roots of the characteristic equation (40) are plotted on the complex plane as done in the earlier cases and is shown in Fig. 5. This plot indicates that the exact BGK–Burnett equations are stable only for very low values of the local Knudsen number. Hence, to stabilize the BGK–Burnett equations, the material derivatives must be expressed in terms of the spatial derivatives.

IV. Boltzmann's H-Theorem

The BGK–Burnett equations must satisfy the second law of thermodynamics. There is, however, no acceptable definition of entropy for a system in a state of nonequilibium. Physical intuition tells us that an isolated system will evolve from an arbitrary initial state to a state of equilibrium. Boltzmann's H-Theorem formalizes this notion and also makes explicit the manner in which this evolution proceeds.

For a spatially inhomogeneous gas,¶¶ Grad[14] has shown that the following inequality must be satisfied when the gas approaches equilibrium:

$$\frac{\partial H}{\partial t} + \frac{\partial H_v}{\partial x} \le 0 \tag{42}$$

where

$$H = \int_{\mathcal{R}} f \ell n f \, \mathrm{d}v_x \tag{43}$$

$$H_v = \int_{\mathcal{R}} v_x f \ell n f \, \mathrm{d}v_x \tag{44}$$

This classical definition of the H-function is based on the assumption that the gas is monatomic, as a result of which the molecules do not have any internal energy. Because the Maxwellian used in the derivation of the BGK–Burnett equations takes into consideration the energy contribution caused by the various nontranslational degrees of freedom, the definition of H must be modified to account for these differences. The modified $\mathcal{H}$ function[13] is obtained by evaluating the moment:

$$\left\langle \left[1 + \ell n f - 2\frac{(5-3\gamma)}{(3-\gamma)}\beta I\right], \frac{\partial f}{\partial t} + v_x\frac{\partial f}{\partial x}\right\rangle$$

$$= \left\langle \left[1 + \ell n f - 2\frac{(5-3\gamma)}{(3-\gamma)}\beta I\right], v\left[f^{(0)} - f\right]\right\rangle \tag{45}$$

For a Maxwellian distribution function,*** the preceding equation takes the form

$$\left\langle \left[1 + \ell n f^{(0)} - 2\frac{(5-3\gamma)}{(3-\gamma)}\beta I\right], \frac{\partial f^{(0)}}{\partial t} + v_x\frac{\partial f^{(0)}}{\partial x}\right\rangle = 0 \tag{46}$$

which can be simplified to

$$\frac{\partial \mathcal{H}^{(0)}}{\partial t} + \frac{\partial \mathcal{H}_v^{(0)}}{\partial x} = 0 \tag{47}$$

where

$$\mathcal{H}^{(0)} = \int_{\mathcal{R}^+}\int_{\mathcal{R}}\left[f^{(0)}\ell n f^{(0)} + \frac{5-3\gamma}{2(\gamma-1)}f^{(0)}\ell n\beta\right]\mathrm{d}v_x\,\mathrm{d}I \tag{48}$$

$$\mathcal{H}_v^{(0)} = \int_{\mathcal{R}^+}\int_{\mathcal{R}} v_x\left[f^{(0)}\ell n f^{(0)} + \frac{5-3\gamma}{2(\gamma-1)}f^{(0)}\ell n\beta\right]\mathrm{d}v_x\,\mathrm{d}I \tag{49}$$

Further, it can be shown that for a Maxwellian distribution function $\rho s^{(0)} = -R\mathcal{H}^{(0)}$, leading to the entropy equation

$$\rho\frac{\mathbf{D}}{\mathbf{D}t}s^{(0)} = 0 \tag{50}$$

On extending the definition of the $\mathcal{H}$ function to higher-order distribution functions, we write

$$\mathcal{H} = \int_{\mathcal{R}^+}\int_{\mathcal{R}}\left[f\ell n f + \frac{5-3\gamma}{2(\gamma-1)}f\ell n\beta\right]\mathrm{d}v_x\,\mathrm{d}I \tag{51}$$

$$\mathcal{H}_v = \int_{\mathcal{R}^+}\int_{\mathcal{R}} v_x\left[f\ell n f + \frac{5-3\gamma}{2(\gamma-1)}f\ell n\beta\right]\mathrm{d}v_x\,\mathrm{d}I \tag{52}$$

Extending the definition of specific entropy s to include expressions for $\mathcal{H}$ resulting from nonequilibrium (higher-order) distribution functions leads to $\rho s = -R\mathcal{H}$, where

¶¶A spatially inhomogeneous gas is defined as one in which the density varies with position.

***It can be shown that $1 + \ell n f^{(0)} - 2[(5-3\gamma)/(3-\gamma)]\beta I$ can be expressed as a linear combination of collision invariants. One can see that the expression for $\mathcal{H}$ reduces to the classical definition of $H = \int_{\mathcal{R}^+}\int_{\mathcal{R}} f\ell n f \, \mathrm{d}v_x \, \mathrm{d}I$ for the specific case of a monatomic gas (i.e., $\gamma = \frac{5}{3}$).

$$s = s^{(0)} + s^{(1)} + s^{(2)} + \cdots, \qquad \mathcal{H} = \mathcal{H}^{(0)} + \mathcal{H}^{(1)} + \mathcal{H}^{(2)} + \cdots \quad (53)$$

On substituting $\rho s = -R\mathcal{H}$ in Eq. (42) and simplifying, we obtain

$$\rho \frac{\mathbf{D}s}{\mathbf{D}t} + \nabla \cdot \boldsymbol{J} = \dot{\sigma} \quad (54)$$

where $\boldsymbol{J}$ denotes the entropy flux and $\dot{\sigma}$ denotes the rate of production of irreversible entropy. In accordance with the second law of thermodynamics, the irreversible entropy produced must be either positive or zero. The entropy flux $\boldsymbol{J}$ and the irreversible entropy production σ can be expressed as

$$\boldsymbol{J} = \boldsymbol{J}^{(0)} + \boldsymbol{J}^{(1)} + \boldsymbol{J}^{(2)} + \cdots, \qquad \dot{\sigma} = \dot{\sigma}^{(0)} + \dot{\sigma}^{(1)} + \dot{\sigma}^{(2)} + \cdots \quad (55)$$

For a Maxwellian distribution function the irreversible entropy produced equals zero ($\dot{\sigma}^{(0)} = 0$). For the Navier–Stokes and BGK–Burnett equations we will show that the irreversible entropy produced is positive by evaluating the following moment of the BGK–Boltzmann equation:

$$\frac{\partial \mathcal{H}}{\partial t} + \frac{\partial \mathcal{H}_v}{\partial x} = \int_{\mathcal{R}^+}\int_{\mathcal{R}} \nu\left[f^{(0)} - f\right] \times \left[1 + \ell n f - \frac{2(5-3\gamma)}{(3-\gamma)}\beta I\right] \mathrm{d}v_x\, \mathrm{d}I \quad (56)$$

and showing that the right-hand side (RHS) of the preceding equation is less than zero for all Knudsen numbers. The first- and second-order distribution functions are given by the expressions

$$f = f^{(0)}\left[1 + \xi\phi^{(1)}\right], \qquad f = f^{(0)}\left[1 + \xi\phi^{(1)} + \xi^2\phi^{(2)}\right] \quad (57)$$

On expressing $\ell n f$ as a Taylor series and considering only terms up to the first power in the Knudsen number, we obtain the approximation

$$\ell n\left\{f^{(0)}\left[1 + \xi\phi^{(1)}\right]\right\} \approx \ell n f^{(0)} + \xi\phi^{(1)} \quad (58)$$

Similarly, retaining terms up to the second power in the Knudsen number yields

$$\ell n\left\{f^{(0)}\left[1 + \xi\phi^{(1)}\right]\right\} \approx \ell n f^{(0)} + \xi\phi^{(1)} + \xi^2\phi^{(2)} - \frac{\left[\xi\phi^{(1)}\right]^2}{2} \quad (59)$$

On substituting Eq. (58) in Eq. (56) and retaining only terms up to the second power in the Knudsen number, the RHS of Eq. (56) takes the form

$$-\int_{\mathcal{R}^+}\int_{\mathcal{R}} \nu\xi\left\{f^{(0)}\phi^{(1)} + \xi f^{(0)}\phi^{(2)} + \xi f^{(0)}\left[\phi^{(1)}\right]^2\right\} \times \left[1 + \ell n f^{(0)} - 2\frac{(5-3\gamma)}{(3-\gamma)}\beta I\right] \mathrm{d}v_x\, \mathrm{d}I \quad (60)$$

On evaluating the moments in Eq. (60) and multiplying by $-R$, we obtain

$$\dot{\sigma} = \dot{\sigma}^{(1)} = \frac{\mu R}{p}\left[\frac{5\rho}{4\beta^3}\left(\frac{\partial\beta}{\partial x}\right)^2 + \frac{(3\gamma^2 - 10\gamma + 11)}{2}\rho\left(\frac{\partial u_x}{\partial x}\right)^2\right] \quad (61)$$

One can see that the preceding expression for the rate of irreversible entropy production is always positive. Hence the Navier–Stokes equations do not violate the second law of thermodynamics. Expanding the RHS of Eq. (56) to the the third power in the Knudsen number yields the additional terms

$$-\int_{\mathcal{R}^+}\int_{\mathcal{R}} \nu\xi^3\left\{2f^{(0)}\phi^{(1)}\phi^{(2)} - f^{(0)}\frac{\left[\phi^{(1)}\right]^3}{2}\right\} \mathrm{d}v_x\, \mathrm{d}I \quad (62)$$

which on evaluating and multiplying by $-R$ yields

$$\begin{aligned}\dot{\sigma}^{(2)} = {} & \frac{\mu^2 R}{p^2}\left(-2\frac{\mathbf{D}}{\mathbf{D}t}\left(\frac{5\rho}{4\beta^3}\frac{\partial\beta}{\partial x}\right)\frac{\partial\beta}{\partial x} - (3\gamma^2 - 10\gamma + 11)\right. \\ & \times \frac{\mathbf{D}}{\mathbf{D}t}\left(\rho\frac{\partial u_x}{\partial x}\right)\frac{\partial u_x}{\partial x} + 6\left(\frac{\theta_4}{4} + \theta_5\right)\frac{\partial}{\partial x}\left(\frac{\rho}{\beta^2}\frac{\partial u_x}{\partial x}\right)\frac{\partial\beta}{\partial x} \\ & - (45\gamma - 91)\frac{\rho}{8\beta^3}\left(\frac{\partial\beta}{\partial x}\right)^2\frac{\partial u_x}{\partial x} - \{(\gamma-1)[3(\gamma-1)^2 + 4]\} \\ & \times \left(\frac{\partial u_x}{\partial x}\right)^3 - 2\left[(3\gamma - 5)\left(\frac{\theta_1}{4} + \frac{\theta_2}{4} + \frac{3\theta_3}{8}\right) + (3-\gamma)\right. \\ & \times \left(\frac{3\theta_1}{4} + \frac{3\theta_2}{4} + \frac{15\theta_3}{8}\right) - (\gamma-1)\left(\frac{\theta_1}{2} + \theta 2 + \frac{3\theta_3}{4}\right)\Bigg] \\ & \left.\times \frac{\partial}{\partial x}\left(\frac{\rho}{\beta^2}\frac{\partial\beta}{\partial x}\right)\frac{\partial u_x}{\partial x}\right)\end{aligned} \quad (63)$$

the irreversible entropy production term caused by the second-order term in the distribution function. The total irreversible entropy produced by the BGK–Burnett equations is $\dot{\sigma} = \dot{\sigma}^{(1)} + \dot{\sigma}^{(2)}$. It can be seen that it is not possible to determine analytically, as in the case of $\dot{\sigma}^{(1)}$ for the Navier–Stokes equations, whether $\dot{\sigma} = \dot{\sigma}^{(1)} + \dot{\sigma}^{(2)}$ is positive for all Knudsen numbers. Hence, computationally we see that for all of the cases considered the BGK–Burnett equations produce a positive irreversible entropy.

V. Hypersonic Shock Structure

The hypersonic shock structure for argon has been computed using the one-dimensional BGK–Burnett equations. The upstream conditions were specified, and the downstream conditions were determined by the Rankine–Hugoniot relations. The flow parameters used are

$$T_\infty = 300\,\mathrm{K}, \qquad P_\infty = 1.01325 \times 10^5\,\mathrm{Nm}^{-2}$$
$$\gamma = 1.6666, \qquad \mu_\infty = 22.7 \times 10^{-6}\,\mathrm{Nm}^{-2} \quad (64)$$

For purposes of comparison, the same flow conditions as Zhong[5] were used for the computations. The Navier–Stokes solution was taken as the initial value for the BGK–Burnett equations. This smooth spatial distribution is imposed on a mesh that corresponds to the expected shock thickness. The length of the control volume enclosing the shock was chosen to be equal to $1000\lambda_\infty$. The mean free path based on the freestream parameters is obtained from

$$\lambda_\infty = \frac{16\mu_\infty}{5\rho_\infty\sqrt{2\pi RT_\infty}} \quad (65)$$

A set of computational experiments was carried out to compare the BGK–Burnett (with stress and heat-transfer terms of $\mathcal{O}(\mu^2)$) with the Burnett solutions of Fiscko and Chapman.[4] A hybrid scheme was used that employed the first-order kinetic wave particle scheme (KWPS)[15] for the Euler part and central differences for the Navier–Stokes and BGK–Burnett flux vectors. Tests were carried out for Mach 20 and 35. To test for instabilities caused by small wavelength disturbances, the number of grid points was increased from 101 to 501. Figures 6–9 show the variations of specific entropy across the shock. The BGK–Burnett equations show a positive entropy change throughout the flowfield, whereas the conventional Burnett equations give rise to a negative entropy spike just ahead of

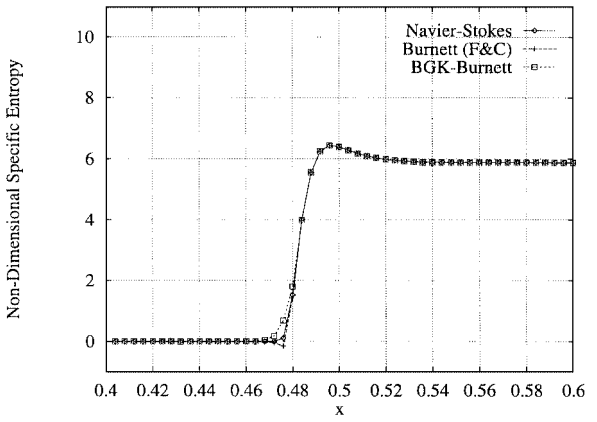

Fig. 6 Specific entropy variation across a Mach 20 normal shock in a monatomic gas (argon), $\Delta x/\lambda_\infty = 8.0$. One-dimensional Euler equations have been used to approximate the material derivatives, i.e., D( )/Dt, in terms of spatial derivatives. This plot shows that the BGK–Burnett equations produce a positive entropy change throughout the flowfield. The conventional Burnett equations have coefficients used by Fiscko and Chapman[4] (F&C).

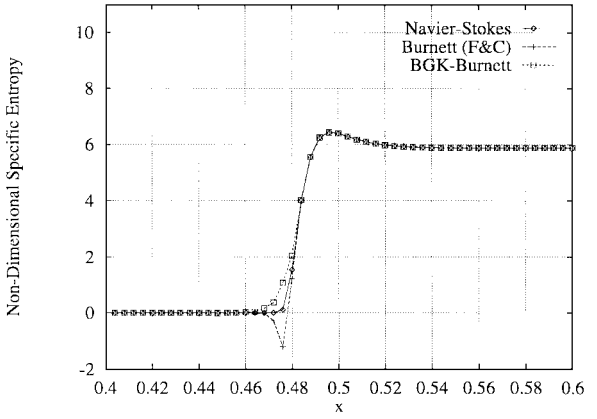

Fig. 7 Specific entropy variation across a Mach 20 normal shock in a monatomic gas (argon), $\Delta x/\lambda_\infty = 4.0$. One-dimensional Euler equations have been used to approximate the material derivatives, i.e., D( )/Dt, in terms of spatial derivatives. This plot shows that the BGK–Burnett equations produce a positive entropy change throughout the flowfield. The conventional Burnett equations have coefficients used by Fiscko and Chapman[4] (F&C).

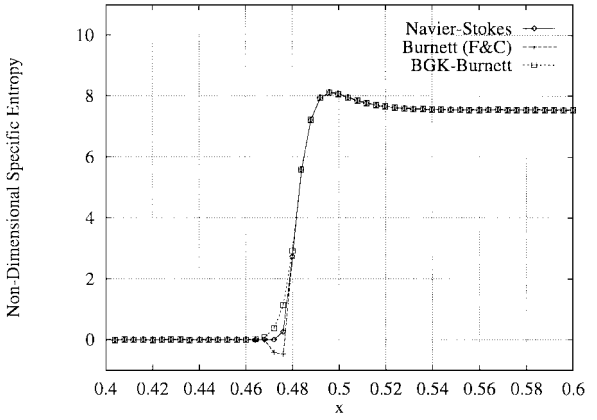

Fig. 8 Specific entropy variation across a Mach 35 normal shock in a monatomic gas (argon), $\Delta x/\lambda_\infty = 8.0$. One-dimensional Euler equations have been used to approximate the material derivatives, i.e., D( )/Dt, in terms of spatial derivatives. This plot shows that the BGK–Burnett equations produce a positive entropy change throughout the flowfield. The conventional Burnett equations have coefficients used by Fiscko and Chapman[4] (F&C).

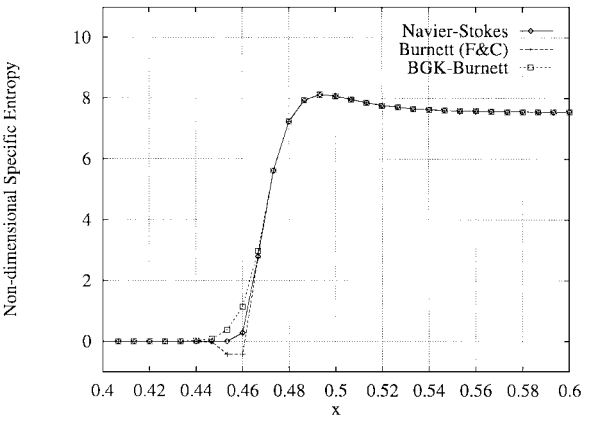

Fig. 9 Specific entropy variation across a Mach 35 normal shock in a monatomic gas (argon), $\Delta x/\lambda_\infty = 4.0$. One-dimensional Euler equations have been used to approximate the material derivatives, i.e., D( )/Dt, in terms of spatial derivatives. This plot shows that the BGK–Burnett equations produce a positive entropy change throughout the flowfield. The conventional Burnett equations have coefficients used by Fiscko and Chapman[4] (F&C).

the shock as the number of grid points is increased. This negative entropy spike increases in magnitude until the conventional Burnett equations break down completely. The BGK–Burnett equations did not exhibit any kind of instability for the range of grid points considered.

VI. Two-Dimensional BGK–Burnett Equations

The two-dimensional BGK–Burnett equations are derived in a manner similar to the derivation of the one-dimensional BGK–Burnett equations explained earlier. The two-dimensional BGK–Boltzmann equation is given by

$$\frac{\partial f}{\partial t} + v_x \frac{\partial f}{\partial x} + v_y \frac{\partial f}{\partial y} = \nu\left[f - f^{(0)}\right] \tag{66}$$

where

$$f = f^{(0)} + \xi f^{(1)} + \xi^2 f^{(2)} \tag{67}$$

denotes the second-order distribution function and

$$f^{(0)} = (\rho/I_0)(\beta/\pi)\exp\left[-I/I_0 - \beta C_x^2 - \beta C_y^2\right] \tag{68}$$

denotes the two-dimensional Maxwellian (equilibrium) distribution.[†††] On substituting Eq. (67) in Eq. (66) and equating like powers of the Knudsen number, we obtain the following equations for the first- and second-order terms of the distribution function:

$$f^{(1)} = -\frac{1}{\xi\nu}\left[\frac{\partial f^{(0)}}{\partial t} + v_x \frac{\partial f^{(0)}}{\partial x} + v_y \frac{\partial f^{(0)}}{\partial y}\right] \tag{69}$$

$$f^{(2)} = -\frac{1}{\xi\nu}\left[\frac{\partial f^{(1)}}{\partial t} + v_x \frac{\partial f^{(1)}}{\partial x} + v_y \frac{\partial f^{(1)}}{\partial y}\right] \tag{70}$$

On expressing $f^{(1)} = f^{(0)}\phi^{(1)}$ and using the Euler equations to express the material derivatives in terms of the spatial derivatives,[10] we obtain

$$\begin{aligned} f^{(1)} = f^{(0)}\phi^{(1)} = -\frac{f^{(0)}}{\xi\nu}\Bigg[&\mathcal{A}^{(1)}(I, C_x, C_y)\frac{\partial\beta}{\partial x} \\ &+ \mathcal{A}^{(2)}(I, C_x, C_y)\frac{\partial\beta}{\partial y} + \mathcal{A}^{(3)}(I, C_x, C_y)\frac{\partial u_x}{\partial x} \\ &+ \mathcal{A}^{(4)}(I, C_x, C_y)\frac{\partial u_y}{\partial y} + \mathcal{A}^{(5)}(I, C_x, C_y)\frac{\partial u_x}{\partial y} \\ &+ \mathcal{A}^{(5)}(I, C_x, C_y)\frac{\partial u_y}{\partial x}\Bigg] \end{aligned} \tag{71}$$

[†††] The average internal energy in two dimensions is given by the equation $I_0 = (2-\gamma)/2\beta(\gamma-1)$.

where

$$\mathcal{A}^{(1)}(I, C_x, C_y) = (3/\beta)C_x - (I/\beta I_0)C_x - C_x C_y^2 - C_x^3 \tag{72}$$

$$\mathcal{A}^{(2)}(I, C_x, C_y) = (3/\beta)C_y - (I/\beta I_0)C_y - C_y C_x^2 - C_y^3 \tag{73}$$

$$\mathcal{A}^{(3)}(I, C_x, C_y) = \beta(3-\gamma)C_x^2 - \beta(\gamma-1)C_y^2 - (\gamma-1)(I/I_0) + (2\gamma-3) \tag{74}$$

$$\mathcal{A}^{(4)}(I, C_x, C_y) = \beta(3-\gamma)C_y^2 - \beta(\gamma-1)C_x^2 - (\gamma-1)(I/I_0) + (2\gamma-3) \tag{75}$$

$$\mathcal{A}^{(5)}(I, C_x, C_y) = 2\beta C_x C_y \tag{76}$$

One can see that the first-order term of the distribution function satisfies the moment relation

$$\left\langle \boldsymbol{\Psi}, \xi f^{(1)} \right\rangle = \left\langle \boldsymbol{\Psi}, \xi f^{(0)} \phi^{(1)} \right\rangle = 0 \tag{77}$$

where the inner product is defined as

$$\left\langle \boldsymbol{\Psi}, \xi f^{(1)} \right\rangle = \int_{\mathcal{R}^+} \int_{\mathcal{R}} \int_{\mathcal{R}} \boldsymbol{\Psi} \xi f^{(1)} \, \mathrm{d}v_x \, \mathrm{d}v_y \, \mathrm{d}I \tag{78}$$

$$\boldsymbol{\Psi} = \left[1, v_x, v_y, \left(I + v_x^2/2 + v_y^2/2\right)\right]^T \tag{79}$$

denotes the collision invariant vector. On substituting Eq. (69) in Eq. (70), we obtain

$$f^{(2)} = -\frac{1}{\xi \nu}\left\{ \frac{\partial}{\partial t}\left[f^{(0)}\phi^{(1)}\right] + \frac{\partial}{\partial x}\left[u_x f^{(0)}\phi^{(1)}\right] + \frac{\partial}{\partial x}\left[C_x f^{(0)}\phi^{(1)}\right] + \frac{\partial}{\partial y}\left[u_y f^{(0)}\phi^{(1)}\right] + \frac{\partial}{\partial y}\left[C_y f^{(0)}\phi^{(1)}\right]\right\} \tag{80}$$

We note, as mentioned earlier, in the derivation of the one-dimensional second-order distribution function that $f^{(2)}$ does not satisfy the moment closure relationship

$$\left\langle \boldsymbol{\Psi}, \xi^2 f^{(2)} \right\rangle = 0 \tag{81}$$

Hence, we need to define some additional terms with closure coefficients that satisfy Eq. (81). An additional constraint was imposed to ensure that the two-dimensional BGK–Burnett equations reduced to the one-dimensional BGK–Burnett equations when the $\partial/\partial y$ terms were set equal to zero. The second-order term in the distribution function is defined as

$$f^{(2)} = -\frac{1}{\xi \nu}\left\{ \frac{\partial}{\partial t}\left[f^{(0)}\phi^{(1)}\right] + \frac{\partial}{\partial x}\left[u_x f^{(0)}\phi^{(1)}\right] + \frac{\partial}{\partial x}\left[f^{(0)}\tilde{\phi}_{(x)}^{(1)}(I, C_x, C_y)\right] + \frac{\partial}{\partial y}\left[u_y f^{(0)}\phi^{(1)}\right] + \frac{\partial}{\partial y}\left[f^{(0)}\tilde{\phi}_{(y)}^{(1)}(I, C_x, C_y)\right]\right\} \tag{82}$$

where

$$\tilde{\phi}_{(x)}^{(1)}(I, C_x, C_y) = -\frac{1}{\xi \nu}\left[\tilde{\mathcal{B}}^{(1)}(I, C_x, C_y)\frac{\partial \beta}{\partial x} + \tilde{\mathcal{B}}^{(2)}(I, C_x, C_y)\frac{\partial \beta}{\partial y} + \tilde{\mathcal{B}}^{(3)}(I, C_x, C_y)\frac{\partial u_x}{\partial x} + \tilde{\mathcal{B}}^{(4)}(I, C_x, C_y)\frac{\partial u_y}{\partial y} + \tilde{\mathcal{B}}^{(5)}(I, C_x, C_y)\frac{\partial u_x}{\partial y}\tilde{\mathcal{B}}^{(5)}(I, C_x, C_y)\frac{\partial u_y}{\partial x}\right] \tag{83}$$

$$\tilde{\phi}_{(y)}^{(1)}(I, C_x, C_y) = -\frac{1}{\xi \nu}\left[\tilde{\mathcal{C}}^{(1)}(I, C_x, C_y)\frac{\partial \beta}{\partial x} + \tilde{\mathcal{C}}^{(2)}(I, C_x, C_y)\frac{\partial \beta}{\partial y} + \tilde{\mathcal{C}}^{(3)}(I, C_x, C_y)\frac{\partial u_x}{\partial x} + \tilde{\mathcal{C}}^{(4)}(I, C_x, C_y)\frac{\partial u_y}{\partial y} + \tilde{\mathcal{C}}^{(5)}(I, C_x, C_y)\frac{\partial u_x}{\partial y}\tilde{\mathcal{C}}^{(5)}(I, C_x, C_y)\frac{\partial u_y}{\partial x}\right] \tag{84}$$

The moment closure functions $\tilde{\mathcal{B}}^{(i)}(I, C_x, C_y)$ and $\tilde{\mathcal{C}}^{(i)}(I, C_x, C_y)$ $\forall i = 1, \ldots, 5$ in Eqs. (83) and (84) are given by the relations

$$\tilde{\mathcal{B}}^{(1)}(I, C_x, C_y) = [(3+\alpha_1)/\beta]C_x^2 - [(1-\alpha_2)/\beta I_0]IC_x^2 - (1+\alpha_3)C_x^2 C_y^2 - (1+\alpha_1)C_x^4 \tag{85}$$

$$\tilde{\mathcal{B}}^{(2)}(I, C_x, C_y) = (3/\beta)C_x C_y - (1/\beta I_0)IC_x C_y - C_x^3 C_y - C_x C_y^3 \tag{86}$$

$$\tilde{\mathcal{B}}^{(3)}(I, C_x, C_y) = \beta[(3-\gamma)+\alpha_4]C_x^3 - \beta[(\gamma-1)+\alpha_5]C_x C_y^2 - \left[\frac{(\gamma-1)+\alpha_4}{I_0}\right]IC_x + [(2\gamma-3)+\alpha_4]C_x \tag{87}$$

$$\tilde{\mathcal{B}}^{(4)}(I, C_x, C_y) = \beta[(3-\gamma)+\alpha_6]C_x C_y^2 - \beta[(\gamma-1)+\alpha_6]C_x^3 - \left[\frac{(\gamma-1)+\alpha_6}{I_0}\right]IC_x + [(2\gamma-3)+\alpha_6]C_x \tag{88}$$

$$\tilde{\mathcal{B}}^{(5)}(I, C_x, C_y) = 2\beta C_x^2 C_y + \alpha_7 \beta^3 C_x^4 C_y^3 \tag{89}$$

$$\tilde{\mathcal{C}}^{(1)}(I, C_x, C_y) = (3/\beta)C_x C_y - (1/\beta I_0)IC_x C_y - C_x C_y^3 - C_x^3 C_y \tag{90}$$

$$\tilde{\mathcal{C}}^{(2)}(I, C_x, C_y) = [(3+\alpha_1)/\beta]C_y^2 - [(1-\alpha_2)/\beta I_0]IC_y^2 - (1+\alpha_3)C_x^2 C_y^2 - (1+\alpha_1)C_y^4 \tag{91}$$

$$\tilde{\mathcal{C}}^{(3)}(I, C_x, C_y) = \beta[(3-\gamma)+\alpha_6]C_x^2 C_y - \beta[(\gamma-1)+\alpha_6]C_y^3 - \left[\frac{(\gamma-1)+\alpha_6}{I_0}\right]IC_y + [(2\gamma-3)+\alpha_6]C_y \tag{92}$$

$$\tilde{\mathcal{C}}^{(4)}(I, C_x, C_y) = \beta[(3-\gamma)+\alpha_4]C_y^3 - \beta[(\gamma-1)+\alpha_5]C_x^2 C_y - \left[\frac{(\gamma-1)+\alpha_4}{I_0}\right]IC_y + [(2\gamma-3)+\alpha_4]C_y \tag{93}$$

$$\tilde{\mathcal{C}}^{(5)}(I, C_x, C_y) = 2\beta C_x C_y^2 + \alpha_7 \beta^3 C_x^3 C_y^4 \tag{94}$$

The closure coefficients α_k $\forall k = 1, \ldots, 7$ are given in the Appendix.

The two-dimensional BGK–Burnett equations are written in the conservation law form as

$$\frac{\partial \boldsymbol{Q}}{\partial t} + \frac{\partial \boldsymbol{G}}{\partial x} + \frac{\partial \boldsymbol{H}}{\partial y} = 0 \tag{95}$$

where $\boldsymbol{G} = \boldsymbol{G}^i + \boldsymbol{G}^v + \boldsymbol{G}^B$ and $\boldsymbol{H} = \boldsymbol{H}^i + \boldsymbol{H}^v + \boldsymbol{H}^B$. The field vector is given by $\boldsymbol{Q} = [\rho, \rho u_x, \rho u_y, \rho e_t]^T$ and the flux vectors are given by the expressions

$$\boldsymbol{G}^i = \begin{bmatrix} \rho u_x \\ p + \rho u_x^2 \\ \rho u_x u_y \\ p u_x + \rho u_x e_t \end{bmatrix}, \qquad \boldsymbol{G}^v = \begin{bmatrix} 0 \\ -\tau_{xx}^v \\ -\tau_{xy}^v \\ -\tau_{xx}^v u_x - \tau_{xy}^v u_y + \dot{q}_x^v \end{bmatrix}$$

$$\boldsymbol{G}^B = \begin{bmatrix} 0 \\ -\tau_{xx}^B \\ -\tau_{xy}^B \\ -\tau_{xx}^B u_x - \tau_{xy}^B u_y + \dot{q}_x^B \end{bmatrix}$$

$$\boldsymbol{H}^i = \begin{bmatrix} \rho u_y \\ \rho u_x u_y \\ p + \rho u_y^2 \\ p u_y + \rho u_y e_t \end{bmatrix}, \qquad \boldsymbol{H}^v = \begin{bmatrix} 0 \\ -\tau_{yx}^v \\ -\tau_{yy}^v \\ -\tau_{yx}^v u_x - \tau_{yy}^v u_y + \dot{q}_y^v \end{bmatrix}$$

$$\boldsymbol{H}^B = \begin{bmatrix} 0 \\ -\tau_{yx}^B \\ -\tau_{yy}^B \\ -\tau_{yx}^B u_x - \tau_{yy}^B u_y + \dot{q}_y^B \end{bmatrix}$$

The two-dimensional Navier–Stokes stress and heat-transfer expressions are given by

$$\tau_{xx}^v = \mu\left[(3-\gamma)\frac{\partial u_x}{\partial x} - (\gamma-1)\frac{\partial u_y}{\partial y}\right] \tag{96}$$

$$\tau_{xy}^v = \mu\left[\frac{\partial u_x}{\partial y} + \frac{\partial u_y}{\partial x}\right] \tag{97}$$

$$\tau_{yy}^v = \mu\left[(3-\gamma)\frac{\partial u_y}{\partial y} - (\gamma-1)\frac{\partial u_x}{\partial x}\right] \tag{98}$$

$$\dot{q}_x^v = -\kappa\frac{\partial T}{\partial x} \tag{99}$$

$$\dot{q}_y^v = -\kappa\frac{\partial T}{\partial y} \tag{100}$$

The two-dimensional BGK–Burnett stress and heat-transfer expressions are given by

$$\begin{aligned}\tau_{xx}^B = \frac{\mu^2}{p^2}\times\Bigg\{&\left(\frac{\rho}{2\beta^2}\frac{\mathbf{D}\beta}{\mathbf{D}t} - \frac{1}{2\beta}\frac{\mathbf{D}\rho}{\mathbf{D}t}\right)\left[(3-\gamma)\frac{\partial u_x}{\partial x} + (1-\gamma)\frac{\partial u_y}{\partial y}\right]\\ &- \frac{\rho}{2\beta}\left[(3-\gamma)\frac{\mathbf{D}}{\mathbf{D}t}\left(\frac{\partial u_x}{\partial x}\right) + (1-\gamma)\frac{\mathbf{D}}{\mathbf{D}t}\left(\frac{\partial u_y}{\partial y}\right)\right]\\ &- \frac{\rho}{2\beta}\left[(3-\gamma)\left(\frac{\partial u_x}{\partial x}\right)^2 + (1-\gamma)\left(\frac{\partial u_y}{\partial y}\right)\left(\frac{\partial u_x}{\partial x}\right)\right]\\ &- \frac{\rho}{2\beta}\left[(3-\gamma)\left(\frac{\partial u_x}{\partial x}\right)\left(\frac{\partial u_y}{\partial y}\right) + (1-\gamma)\left(\frac{\partial u_y}{\partial y}\right)^2\right]\\ &- \frac{\partial}{\partial x}\left(\frac{\rho\theta_1}{\beta^3}\frac{\partial\beta}{\partial x}\right) - \frac{\partial}{\partial y}\left(\frac{\rho\theta_8}{\beta^3}\frac{\partial\beta}{\partial y}\right)\Bigg\}\end{aligned} \tag{101}$$

$$\begin{aligned}\tau_{xy}^B = \frac{\mu^2}{p^2}\times\Bigg\{&\left(\frac{\rho}{2\beta^2}\frac{\mathbf{D}\beta}{\mathbf{D}t} - \frac{1}{2\beta}\frac{\mathbf{D}\rho}{\mathbf{D}t}\right)\left(\frac{\partial u_x}{\partial y} + \frac{\partial u_y}{\partial x}\right)\\ &- \frac{\rho}{2\beta}\left[\frac{\mathbf{D}}{\mathbf{D}t}\left(\frac{\partial u_x}{\partial y}\right) + \frac{\mathbf{D}}{\mathbf{D}t}\left(\frac{\partial u_y}{\partial x}\right)\right] - \frac{\rho}{2\beta}\left(\frac{\partial u_x}{\partial y}\frac{\partial u_x}{\partial x}\right.\\ &\left. + \frac{\partial u_y}{\partial x}\frac{\partial u_x}{\partial x}\right) - \frac{\rho}{2\beta}\left(\frac{\partial u_x}{\partial y}\frac{\partial u_y}{\partial y} + \frac{\partial u_y}{\partial x}\frac{\partial u_y}{\partial y}\right) + \frac{\partial}{\partial x}\left(\frac{\rho}{4\beta^3}\frac{\partial\beta}{\partial y}\right)\\ &+ \frac{\partial}{\partial y}\left(\frac{\rho}{4\beta^3}\frac{\partial\beta}{\partial x}\right)\Bigg\}\end{aligned} \tag{102}$$

$$\begin{aligned}\tau_{yy}^B = \frac{\mu^2}{p^2}\times\Bigg\{&\left(\frac{\rho}{2\beta^2}\frac{\mathbf{D}\beta}{\mathbf{D}t} - \frac{1}{2\beta}\frac{\mathbf{D}\rho}{\mathbf{D}t}\right)\left[(1-\gamma)\frac{\partial u_x}{\partial x}\right.\\ &\left. + (3-\gamma)\frac{\partial u_y}{\partial y}\right] - \frac{\rho}{2\beta}\left[(1-\gamma)\frac{\mathbf{D}}{\mathbf{D}t}\left(\frac{\partial u_x}{\partial x}\right)\right.\\ &\left. + (3-\gamma)\frac{\mathbf{D}}{\mathbf{D}t}\left(\frac{\partial u_y}{\partial y}\right)\right] - \frac{\rho}{2\beta}\left[(1-\gamma)\left(\frac{\partial u_x}{\partial x}\right)^2\right.\\ &\left. + (3-\gamma)\left(\frac{\partial u_y}{\partial y}\right)\left(\frac{\partial u_x}{\partial x}\right)\right] - \frac{\rho}{2\beta}\left[(1-\gamma)\left(\frac{\partial u_x}{\partial x}\right)\left(\frac{\partial u_y}{\partial y}\right)\right.\\ &\left. + (3-\gamma)\left(\frac{\partial u_y}{\partial y}\right)^2\right] - \frac{\partial}{\partial x}\left(\frac{\rho\theta_8}{\beta^3}\frac{\partial\beta}{\partial x}\right) - \frac{\partial}{\partial y}\left(\frac{\rho\theta_1}{\beta^3}\frac{\partial\beta}{\partial y}\right)\Bigg\}\end{aligned} \tag{103}$$

$$\begin{aligned}\dot{q}_x^B = -\frac{\mu^2}{p^2}\frac{1}{4\beta^3}\frac{\gamma}{(\gamma-1)}\Bigg[&\frac{\mathbf{D}\rho}{\mathbf{D}t}\frac{\partial\beta}{\partial x} - \frac{3\rho}{\beta}\frac{\partial\beta}{\partial x}\frac{\mathbf{D}\beta}{\mathbf{D}t} + \frac{\mathbf{D}}{\mathbf{D}t}\left(\frac{\partial\beta}{\partial x}\right)\\ &+ \frac{\partial\beta}{\partial x}\frac{\partial u_y}{\partial y} + \frac{\partial\beta}{\partial x}\frac{\partial u_x}{\partial x}\Bigg] + \frac{\mu^2}{p^2}\frac{\rho}{2\beta}\Bigg\{\Bigg[(3-\gamma)\frac{\partial u_x}{\partial x} + (1-\gamma)\\ &\times\frac{\partial u_y}{\partial y}\Bigg]\frac{\mathbf{D}u_x}{\mathbf{D}t} + \left[\frac{\partial u_x}{\partial y} + \frac{\partial u_y}{\partial x}\right]\frac{\mathbf{D}u_y}{\mathbf{D}t}\Bigg\} + \frac{\mu^2}{p^2}\times\Bigg\{\frac{\rho\theta_1}{\beta^3}\frac{\partial\beta}{\partial x}\frac{\partial u_x}{\partial x}\\ &- \frac{\rho}{4\beta^3}\frac{\partial\beta}{\partial y}\frac{\partial u_y}{\partial x} + \frac{\partial}{\partial x}\left[\frac{\rho}{\beta^2}(\theta_2+\theta_3+\theta_4)\frac{\partial u_x}{\partial x}\right] + \frac{\partial}{\partial x}\left[\frac{\rho}{\beta^2}(\theta_5\right.\\ &\left.+\theta_6+\theta_7)\frac{\partial u_y}{\partial y}\right]\Bigg\} + \frac{\mu^2}{p^2}\Bigg\{\frac{\rho\theta_8}{\beta^3}\frac{\partial\beta}{\partial y}\frac{\partial u_x}{\partial y} - \frac{\rho}{4\beta^3}\frac{\partial\beta}{\partial x}\frac{\partial u_y}{\partial y}\\ &+ \frac{\partial}{\partial y}\left[\frac{\rho}{\beta^2}2\theta_9\left(\frac{\partial u_x}{\partial y} + \frac{\partial u_y}{\partial x}\right)\right]\Bigg\}\end{aligned} \tag{104}$$

$$\begin{aligned}\dot{q}_y^B = -\frac{\mu^2}{p^2}\frac{1}{4\beta^3}\frac{\gamma}{(\gamma-1)}\Bigg[&\frac{\mathbf{D}\rho}{\mathbf{D}t}\frac{\partial\beta}{\partial y} - \frac{3\rho}{\beta}\frac{\partial\beta}{\partial y}\frac{\mathbf{D}\beta}{\mathbf{D}t} + \frac{\mathbf{D}}{\mathbf{D}t}\left(\frac{\partial\beta}{\partial y}\right)\\ &+ \frac{\partial\beta}{\partial y}\frac{\partial u_x}{\partial x} + \frac{\partial\beta}{\partial y}\frac{\partial u_y}{\partial y}\Bigg] + \frac{\mu^2}{p^2}\frac{\rho}{2\beta}\Bigg\{\Bigg[(1-\gamma)\frac{\partial u_x}{\partial x} + (3-\gamma)\\ &\times\frac{\partial u_y}{\partial y}\Bigg]\frac{\mathbf{D}u_y}{\mathbf{D}t} + \left[\frac{\partial u_x}{\partial y} + \frac{\partial u_y}{\partial x}\right]\frac{\mathbf{D}u_x}{\mathbf{D}t}\Bigg\} + \frac{\mu^2}{p^2}\Bigg(\frac{\rho\theta_8}{\beta^3}\frac{\partial\beta}{\partial x}\frac{\partial u_y}{\partial x}\\ &+ \frac{\rho\theta_1}{\beta^3}\frac{\partial\beta}{\partial y}\frac{\partial u_y}{\partial y} - \frac{\rho}{4\beta^3}\frac{\partial\beta}{\partial y}\frac{\partial u_x}{\partial x} - \frac{\rho}{4\beta^3}\frac{\partial\beta}{\partial x}\frac{\partial u_x}{\partial y}\Bigg) + \frac{\mu^2}{p^2}\\ &\times\Bigg\{\frac{\partial}{\partial x}\left[\frac{\rho}{\beta^2}2\theta_9\left(\frac{\partial u_x}{\partial y} + \frac{\partial u_y}{\partial x}\right)\right] + \frac{\partial}{\partial y}\left[\frac{\rho}{\beta^2}(\theta_5+\theta_6\right.\\ &\left.+\theta_7)\frac{\partial u_x}{\partial x}\right] + \frac{\partial}{\partial y}\left[\frac{\rho}{\beta^2}(\theta_2+\theta_3+\theta_4)\frac{\partial u_y}{\partial y}\right]\Bigg\}\end{aligned} \tag{105}$$

The material derivatives can be expressed in terms of the spatial derivatives by using the Navier–Stokes equations. These resulting expressions have terms that are of $\mathcal{O}(\mu^2)$ and $\mathcal{O}(\mu^3)$ as shown in the one-dimensional BGK–Burnett stress and heat-transfer terms, Eqs. (23) and (24). The derivation of these expressions is straightforward and is not given here because of space limitations.

VII. Blunt-Body Computations

The two-dimensional BGK–Burnett equations were applied to compute the hypersonic flow past a cylindrical leading edge of varying nose radii to simulate different freestream Knudsen numbers.

The Steger–Warming flux-vector splitting was applied to the inviscid flux terms. The Navier–Stokes and BGK–Burnett flux vectors were central differenced. The results of the computations are compared with the results of the augmented Burnett and Navier–Stokes equations.

For the blunt-body flowfield computations freestream conditions were used along the outer boundary. First-order extrapolation of the interior data was used to determine the flow properties along the exit boundary, symmetry boundary conditions were applied to the stagnation streamline, and the first-order Maxwell–Smoluchowski slip boundary conditions were used on the wall surface. The Maxwell–Smoluchowski slip boundary conditions are given by

$$u_s = \frac{2-\bar{\sigma}}{\bar{\sigma}}\bar{l}\left(\frac{\partial u_x}{\partial y}\right)_s + \frac{3}{4}\frac{\mu}{\rho T}\left(\frac{\partial T}{\partial x}\right)_s$$

$$T_s = T_w + \frac{2-\bar{\alpha}}{\bar{\alpha}}\frac{2\gamma}{\gamma+1}\frac{\bar{l}}{Pr}\left(\frac{\partial T}{\partial y}\right)_s \tag{106}$$

where

$$\bar{l} = (2\mu/\rho)\sqrt{\pi/8RT} \tag{107}$$

The subscript s denotes the flow variables on the surface of the body. The reflection coefficient $\bar{\sigma}$ and accomodation coefficient $\bar{\alpha}$ are assumed to be equal to unity.

The two-dimensional BGK–Burnett equations were applied to compute the hypersonic flowfield over a cylindrical leading edge of nose radii 2 and 0.2 m corresponding to freestream Knudsen numbers $Kn_\infty = 0.001$ and 0.01, respectively. The flow conditions used for the computations are

$$M_\infty = 10.0, \qquad Re_\infty = 167.9, \qquad P_\infty = 2.3881\ \text{Nm}^{-2}$$

$$T_\infty = 208.4\ \text{K}, \quad T_w = 1000\ \text{K}, \quad R = 287.04\ \text{m}^2/(\text{s}^2\text{K})$$

$$\gamma = 1.4, \qquad Pr = 0.72 \tag{108}$$

The coefficient of viscosity is calculated using Sutherland's law:

$$\mu = c_1\left[T^{\frac{3}{2}}/(T+c_2)\right] \tag{109}$$

where

$$c_1 = 1.458 \times 10^6\ \text{kg}/(\text{smK}^{\frac{1}{2}}), \qquad c_2 = 110.4\ \text{K} \tag{110}$$

VIII. Results and Discussion of Blunt-Body Computations

A. Case 1: ($Kn_\infty = 0.01$)

The grid used for the computations is shown in Fig. 10. Comparisons of density, velocity, and temperature changes along the stagnation streamline between the two-dimensional Navier–Stokes, the two-dimensional augmented Burnett, and two-dimensional BGK–Burnett solutions are shown in Figs. 11–13, respectively. The density and temperature contours of the Navier–Stokes, augmented Burnett, and BGK–Burnett solutions are shown in Figs. 14–19. The resulting curves of the BGK–Burnett and augmented Burnett solutions are almost coincident. However, differences are observed ahead of the shock, where the velocity curve of the BGK–Burnett solution shows an unexpected peak.

B. Case 2: ($Kn_\infty = 0.001$)

At this small Knudsen number (continuum regime) the solutions of the three sets of equations are identical. Figures 20–22 show the variations of density, velocity, and temperature along the stagnation streamline. This solution indicates that the BGK–Burnett equations do indeed reduce to the Navier–Stokes equations in the continuum limit, thereby satisfying one of the requirements of the extended set of governing equations.

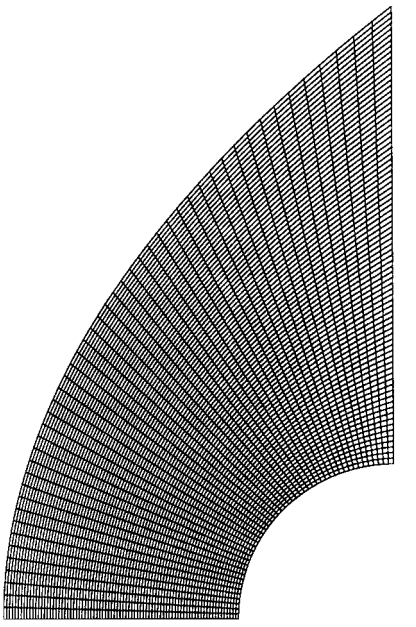

Fig. 10 50 × 82 grid used to compute the blunt-body flow in case 1.

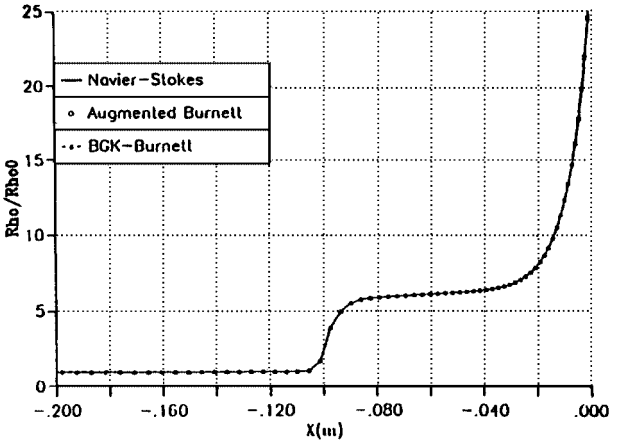

Fig. 11 Density along the stagnation streamline for case 1 (Kn_∞ = 0.01).

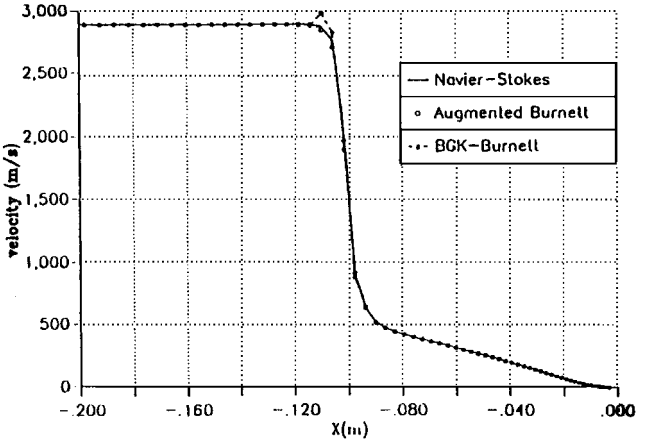

Fig. 12 Velocity along the stagnation streamline for case 1 (Kn_∞ = 0.01).

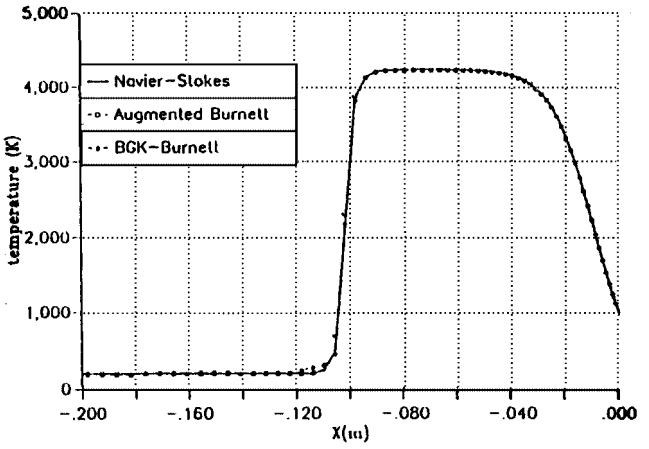

Fig. 13 Temperature along the stagnation streamline for case 1 ($Kn_\infty = 0.01$).

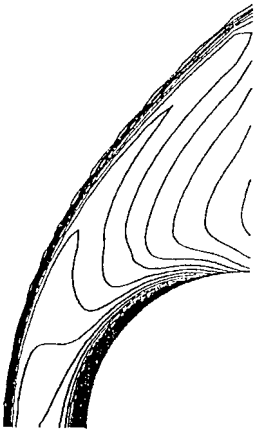

Fig. 14 Navier-Stokes density contours for case 1 ($Kn_\infty = 0.01$).

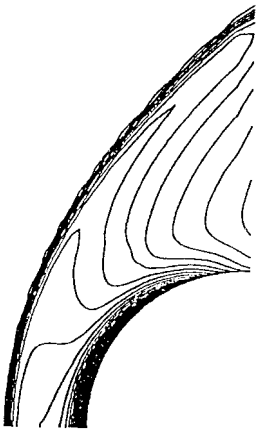

Fig. 15 Augmented Burnett density contours for case 1 ($Kn_\infty = 0.01$).

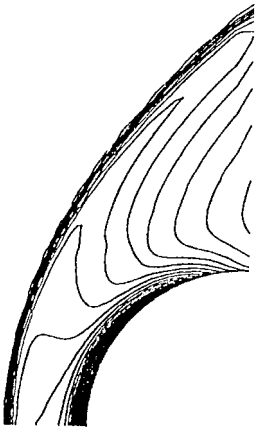

Fig. 16 BGK-Burnett density contours for case 1 ($Kn_\infty = 0.01$).

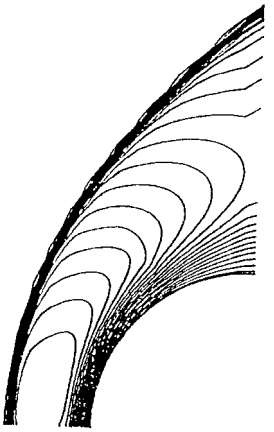

Fig. 17 Navier-Stokes temperature contours for case 1 ($Kn_\infty = 0.01$).

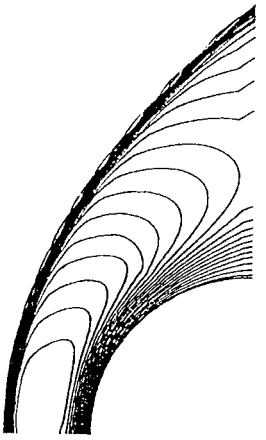

Fig. 18 Augmented Burnett temperature contours for case 1 ($Kn_\infty = 0.01$).

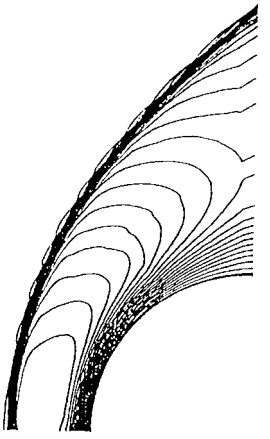

Fig. 19 BGK-Burnett temperature contours for case 1 ($Kn_\infty = 0.01$).

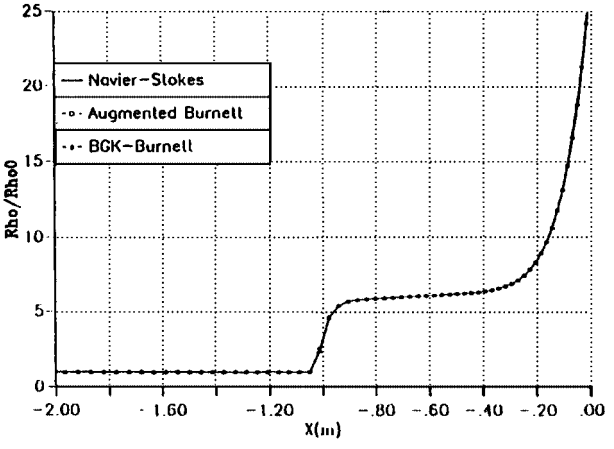

Fig. 20 Density along the stagnation streamline for case 2 ($Kn_\infty = 0.001$).

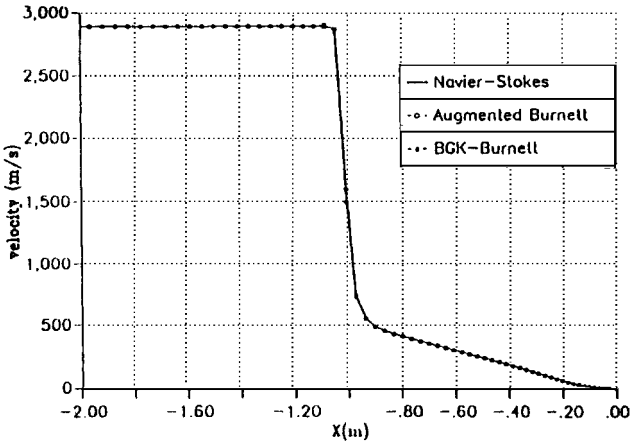

Fig. 21 Velocity along the stagnation streamline for case 2 (Kn_∞ = 0.001).

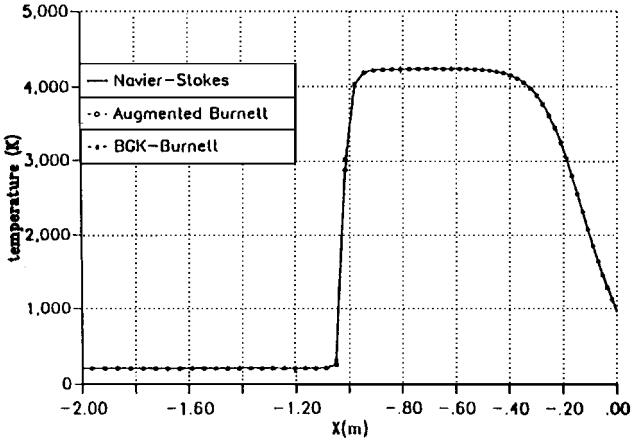

Fig. 22 Temperature along the stagnation streamline for case 2 (Kn_∞ = 0.001).

IX. Conclusions

An entropy consistent set of BGK–Burnett equations has been derived from first principles. The one-dimensional BGK–Burnett equations have been numerically integrated to compute the hypersonic shock structure. The equations are computationally stable for the range of grid points for which results are presented.

The two-dimensional BGK–Burnett equations have been applied to compute the flowfield at $Kn_\infty = 0.001$ and 0.01. At low Knudsen numbers the Navier–Stokes and BGK–Burnett solutions are almost identical. The two-dimensional BGK–Burnett equations are once again stable for the range of Knudsen numbers for which computations have been carried out. Because the BGK–Burnett equations have been shown to be entropy consistent (in one dimension) and satisfy Boltzmann's H-theorem, they are recommended as a extended set of hydrodynamic equations for computing hypersonic flows in the continuum-transition regime.

Appendix: BGK–Burnett Equations

One-Dimensional BGK–Burnett Coefficients

The one-dimensional BGK–Burnett moment closure coefficients are

$$\theta_1 = \frac{5}{2} + \omega_1, \qquad \theta_2 = \omega_2 - 1$$

$$\theta_3 = -(1 + \omega_1), \qquad \theta_4 = (3 - \gamma) + \omega_3$$

$$\theta_5 = -[(\gamma - 1) + \omega_3], \qquad \theta_6 = \frac{3\gamma - 5}{2} + \omega_3$$

$$\omega_1 = \frac{4\gamma}{(9 - 7\gamma)}, \qquad \omega_2 = \frac{2\gamma}{(9 - 7\gamma)}, \qquad \omega_3 = -\frac{2}{3}(3 - \gamma) \tag{A1}$$

Two-Dimensional BGK–Burnett Coefficients

Moment Closure Coefficients

The moment closure coefficients in the two-dimensional second-order distribution function are

$$\Omega_1 = \frac{3 - \gamma}{2}, \qquad \Omega_2 = \frac{3}{4}\left(\theta_1 + \theta_2 + \frac{5}{2}\theta_3\right)$$

$$\Omega_3 = \frac{\gamma}{4(\gamma - 1)}$$

$$\Omega_4 = \frac{1}{8(\gamma - 1)}[\theta_4(6\gamma - 3) + \theta_5(\gamma + 3) + \theta_6(2\gamma)] \tag{A2}$$

Stress and Heat Transfer Coefficients

The coefficients in the two-dimensional BGK–Burnett stress and heat-transfer terms are

$$\theta_1 = \frac{3}{8}[(1 - 3\alpha_1) - 2(1 - \alpha_2) - (1 + \alpha_3)]$$

$$\theta_2 = \frac{2 - \gamma}{8(\gamma - 1)}[(8 - 4\gamma) + (\alpha_4 - \alpha_5)]$$

$$\theta_3 = \frac{1}{16}[(36 - 12\gamma) + (15\alpha_4 - 3\alpha_5)]$$

$$\theta_4 = \frac{1}{16}[(8 - 4\gamma) + 3(\alpha_4 - \alpha_5)]$$

$$\theta_5 = \frac{2 - \gamma}{2(\gamma - 1)}\left\{\frac{1}{4}[(3 - \gamma) + \alpha_6] - \frac{7}{4}[(\gamma - 1) + \alpha_6] + \frac{1}{2}[(2\gamma - 3) + \alpha_6]\right\}$$

$$\theta_6 = \frac{3}{16}[(3 - \gamma) + \alpha_6] - \frac{21}{16}[(\gamma - 1) + \alpha_6] + \frac{3}{8}[(2\gamma - 3) + \alpha_6]$$

$$\theta_7 = \frac{3}{16}[(3 - \gamma) + \alpha_6] - \frac{5}{16}[(\gamma - 1) + \alpha_6] + \frac{1}{8}[(2\gamma - 3) + \alpha_6]$$

$$\theta_8 = \frac{1}{8}(-\alpha_1 + 2\alpha_2 - 3\alpha_3 - 2), \qquad \theta_9 = \frac{3}{8}\left(1 + \frac{15}{8}\alpha_7\right) \tag{A3}$$

Acknowledgments

This work has been supported by the U.S. Air Force Office of Scientific Research Contract F49620-1-0125. The authors wish to acknowledge Len Sakell for his support and encouragement on this project.

References

[1] Bird, G. A., *Molecular Gas Dynamics and the Direct Simulation of Gas Flows*, Oxford Univ. Press, 1994.

[2] Burnett, D., "The Distribution of Velocities and Mean Motion in a Slightly Non-Uniform Gas" *Proceedings of the London Mathematics Society*, Vol. 39, No. 2, 1935, pp. 382–435.

[3] Chapman, S., and Cowling, T. G., *The Mathematical Theory of Non-Uniform Gases*, Cambridge Univ. Press, 1960.

[4] Fiscko, K. A., and Chapman, D. R., "Comparison of Burnett, Super-Burnett and Monte-Carlo Solutions for Hypersonic Shock Structure," Vol. 118, Progress in Aeronautics and Astronautics, AIAA, Washington, DC, 1989, pp. 374–395.

[5] Zhong, X., "Development and Computation of Continuum Higher-Order Constitutive Relations for High Altitude Hypersonic Flow," Ph.D. Dissertation, Dept. of Aeronautics and Astronautics, Stanford Univ., CA, Aug. 1991.

[6] Bobylev, A. V., "The Chapman-Enskog and Grad Methods for Solving the Boltzmann Equation," *Soviet Physics—Doklady*, Vol. 27, No. 1, 1982.

[7]Welder, W. T., Chapman, D. R., and MacCormack, R. W., "Evaluation of Various Forms of the Burnett Equations," AIAA Paper 93-3094, July 1993.

[8]Comeaux, K. A., Chapman, D. R., and MacCormack, R. W., "An Analysis of the Burnett Equations Based on the Second Law of Thermodynamics," AIAA Paper 95-0415, Jan. 1995.

[9]Bhatnagar, P. L., Gross, E. P., and Krook, M., "Model for Collision Processes in Gases, I. Small Amplitude Processes in Charged and Neutral One-Component Systems," *Physical Review*, Vol. 94, No. 3, 1954, pp. 511–524.

[10]Balakrishnan, R., and Agarwal, R. K., "A Kinetic Theory Based Scheme for the Numerical Solution of the BGK–Burnett Equations for Hypersonic Flows in the Continuum-Transition Regime," AIAA Paper 96-0602, Jan. 1996.

[11]Balakrishnan, R., and Agarwal, R. K., "Entropy Consistent Formulation and Numerical Simulation of the BGK–Burnett Equations for Hypersonic Flows in the Continuum-Transition Regime," International Conf. for the Numerical Methods in Fluid Dynamics, Monterey, CA, June 1996.

[12]Balakrishnan, R., and Agarwal, R. K., "Numerical Simulation of the BGK-Burnett for Hypersonic Flows," *Journal of Thermophysics and Heat Transfer*, Vol. 11, No. 3, 1997.

[13]Deshpande, S. M., "On the Maxwellian Distribution, Symmetric Form and Entropy Conservation for the Euler Equations," NASA TP 2583, 1986.

[14]Grad, H., "On the Kinetic Theory of Rarefied Gases," *Communications on Pure and Applied Mechanics*, Vol. 2, 1949, pp. 331–407.

[15]Acheson, K. E., and Agarwal, R. K., "A Kinetic Theory Based Wave Particle Flux Splitting Scheme for Euler Equations," AIAA Paper 95-2178, 1995.